PROCEEDINGS A

royalsocietypublishing.org/journal/rspa

Review

Cite this article: Gallet A, Rigby S, Tallman TN, Kong X, Hajirasouliha I, Liew A, Liu D, Chen L, Hauptmann A, Smyl D. 2022 Structural engineering from an inverse problems perspective. *Proc. R. Soc. A* **478**: 20210526. https://doi.org/10.1098/rspa.2021.0526

Received: 2 September 2021
Accepted: 7 December 2021

Subject Areas:
structural engineering

Keywords:
inverse problems, machine learning, non-destructive testing and evaluation, smart materials and structures, structural design, structural engineering

Author for correspondence:
D. Smyl
e-mail: dsmyl@southalabama.edu

Structural engineering from an inverse problems perspective

A. Gallet[1], S. Rigby[1], T. N. Tallman[2], X. Kong[3], I. Hajirasouliha[1], A. Liew[1], D. Liu[4], L. Chen[1], A. Hauptmann[5,6] and D. Smyl[7]

[1]Department of Civil and Structural Engineering, University of Sheffield, Sheffield, UK
[2]School of Aeronautics and Astronautics, Purdue University, West Lafayette, IN, USA
[3]Department of Physics and Engineering Science, Coastal Carolina University, Conway, SC, USA
[4]School of Physical Sciences, University of Science and Technology of China, Hefei, People's Republic of China
[5]Research Unit of Mathematical Sciences, University of Oulu, Oulu, Finland
[6]Department of Computer Science, University College London, London, UK
[7]Department of Civil, Coastal, and Environmental Engineering, University of South Alabama, Mobile, AL, USA

AG, 0000-0003-4939-9916; XK, 0000-0001-5134-7432; AH, 0000-0002-3756-8121; DS, 0000-0002-6730-5277

The field of structural engineering is vast, spanning areas from the design of new infrastructure to the assessment of existing infrastructure. From the onset, traditional entry-level university courses teach students to analyse structural responses given data including external forces, geometry, member sizes, restraint, etc.—characterizing a *forward* problem (structural causalities → structural response). Shortly thereafter, junior engineers are introduced to structural design where they aim to, for example, select an appropriate structural form for members based on design criteria, which is the *inverse* of what they previously learned. Similar inverse realizations also hold true in structural health monitoring and a number of structural engineering sub-fields (response → structural causalities). In this light, we aim to

THE ROYAL SOCIETY PUBLISHING

demonstrate that many structural engineering sub-fields may be fundamentally or partially viewed as *inverse problems* and thus benefit via the rich and established methodologies from the inverse problems community. To this end, we conclude that the future of inverse problems in structural engineering is inexorably linked to engineering education and machine learning developments.

1. Introduction

The estimation of structural response from loading and boundary conditions is a fundamental concept in structural analysis, from elementary Euler–Bernoulli beam theory to nonlinear simulations involving complex structures subjected to extreme earthquake excitation. In fact, numerical computation of structural responses from known causalities characterizes a *forward* problem (cause → effect) and has rightly been the source of significant research since the advent of modern computing. Among the myriad of computational frameworks, the finite-element method (FEM) [1–4], finite difference [5,6], spectral element [7,8] and hybridizations [9] have proven both widely applicable and successful over the years. The implementation of such forward models has aided engineers in their ability to model, analyse and design structures with arbitrary geometry and precision, contributing greatly to the presence of skyscrapers, supersonic aircraft, large cruise ships and many more engineering examples. In the near future, the pervasiveness of, for example, the FEM appears inevitable while its usefulness is unquestionable in structural engineering applications.

Pragmatically, however, the final configuration of structural members is not known at the beginning of the design process, i.e. one iteration of a structural simulation is not generally sufficient in a real project. This reality implies that the design of structures is an iterative process—for example, the identification of appropriately sized structural members, connections and restraints (causalities) from design constraints, building codes and environmental considerations (data). As is often the case, the iterative design process is carried out initially using design tables, rules of thumb, handcrafted protocols, optimization regimes, etc. Nonetheless, this process is emphatically an *inverse problem*, where an engineer is given data alongside design objectives and challenged to determine the appropriate structural configuration (causalities).

Of course, the field of structural engineering is diverse, in which structural design is one of many sub-fields where inverse problems are applicable. Perhaps a more straightforward implementation of inverse problems is structural health monitoring (SHM), where real-time (or near real-time) data are used in the prognosis of structural condition. Indeed, the detection, localization, prediction and prognosis of potential damage processes are enabled in one of two ways: (i) via pattern recognition or (ii) by solving an inverse problem (or series of inverse problems) [10]. Moreover, certain non-destructive evaluation (NDE) approaches are also known to employ inverse problems (e.g. X-ray computed tomography and emerging NDE approaches in academia) to assess the damage state of structural elements measured offline [11]. For contextualization, a schematic example contrasting the differences between forward and inverse models is provided in figure 1; this well-known problem is referred to as an *inverse elasticity problem*.

These, and many more sub-fields of structural engineering and structural mechanics [12], not only can be (fundamentally or partially) viewed as inverse problems, but also, as we aim to illustrate herein, can benefit from the systematic approaches constituting the rich area of inverse problems. Too often overlooked by structural engineers and structural researchers, the mathematics of inverse problems is an established field, ranging from classical statistical/Bayesian methodology [13] to cutting-edge implementation of deep neural networks [14]. Moreover, while the present use of inverse problem methodologies in structural engineering is limited, its potential is immense across the expanse of the structural engineering sub-fields.

In this paper, this potential will be discussed in detail and contextualized among a broad suite of existing inversion-based applications. To begin, a clear description of inverse problems and

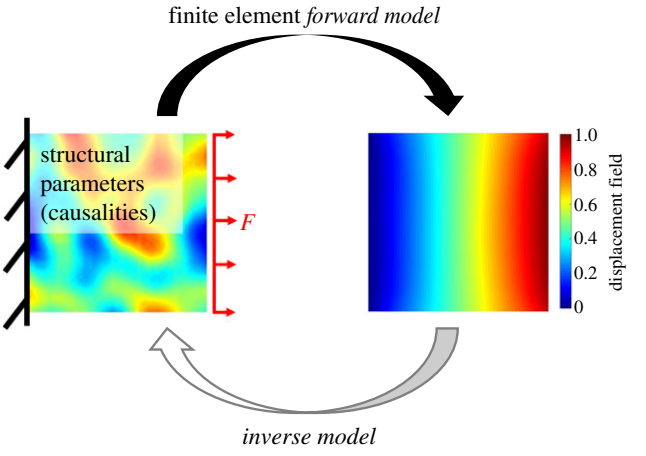

Figure 1. Schematic illustration depicting the forward and inverse problem relationship for a stretched elastic plate with randomized stiffness properties. The forward finite-element model inputs (causalities) are shown as the non-homogeneous stiffness properties while the model output is the displacement field. By contrast, the inverse model aims to estimate the stiffness properties given the displacement field. (Online version in colour.)

methods will be detailed. Following this, a review and discussion of inverse methodologies in modern structural engineering applications will be provided. Inasmuch, the intent of this paper is to examine the following topics in structural engineering through the lens of inverse problems. We remark, however, that the forthcoming topical sections are *not* intended to be exhaustive reviews, but, rather, to provide substantiating evidence for the pervasiveness of inverse problems in structural engineering. Lastly, realizations, overview, paths forward and conclusions will be presented.

2. Inverse problems, methods and contemporary use

Traditionally, the field of inverse problems is concerned with the mathematical question of if and how one can determine the cause for certain measurements. Despite being primarily mathematically oriented, the underlying questions always stem from relevant physics and engineering applications. This is especially true for one of the most prototypical inverse problems, the so-called Calderón problem [15], which asks: Can one determine the conductivity of a body from electrical measurements at the boundary? In fact, this question arose during Calderón's time as a civil engineer, before he pursued an academic career in mathematics. In the following, we want to close the loop back to civil and structural engineering application that once motivated an entire field of mathematical studies, by using the insights gained in the last decades.

More generally speaking, inverse problems consist of finding the unknown characteristics of a structural system from some of the outputs, or measurements, of that system. Most notably, this includes the above-mentioned inverse conductivity problem in geophysics [16] and engineering, but also includes a large field with applications in medical image reconstruction [17,18]. Mathematically, such problems are ill-posed, broadly meaning that the parameters to be estimated, θ, are highly sensitive to changes in the measurement data, d. The solution to the inverse problem involves estimating the parameter θ from a fixed set of measured data d, in contrast to the forward problem of computing d from knowledge of the system parameter θ. Specifically, this means, given the forward model U, which models the system equations, we first formulate the underlying observation model

$$d = U(\theta) + \delta d. \tag{2.1}$$

Here, δd denotes an error term, modelling several sources of possible errors, such as inaccurate measurements or even inaccuracies in the model simulation. The question that remains is: How can we obtain θ from d given the above relationship?; we will call this the reconstruction problem in the following. It is important to note that we cannot simply invert the forward problem (2.1), as the ill-posed nature implies that there can be either no or multiple solutions and additionally under inevitable measurement noise these solutions are not stable to compute by direct inversion. This ill-posedness of the inversion procedure constitutes the underlying paradigm of an *inverse problem*.

In order to obtain stable reconstructions, we make use of a concept known as regularization [19], which aims to assign a unique solution to each set of measurements in a stable manner; this means that if the noise in the measurement vanishes, we would obtain the original system parameter. We can separate such stable reconstruction procedures into two primary classes: those that compute a solution θ^* directly from measured data and those that iteratively aim to fit a solution by minimizing a suitable cost functional. In the first case, we aim to formulate an inverse mapping $U^\dagger$, such that

$$U^\dagger(d) \approx \theta. \tag{2.2}$$

The primary problem in obtaining such direct inversion algorithms is that they can be highly dependent on the problem under consideration. This is especially so when the relationship between d and θ is nonlinear. Thus, obtaining such a mapping is a highly non-trivial task, but reveals much about the underlying problem characteristics and hence is a primary interest of mathematical research [17,20,21].

The second case is a more principled approach that can be formulated for a large class of problems. The underlying premise is to reformulate the reconstruction problem as an optimization problem. That is, we formulate a cost functional that measures how well our reconstruction fits the data while simultaneously enforcing some additional characteristics and acting as regularization for the reconstruction process. Specifically, the reconstruction problem can then be written as finding a minimizer of

$$\theta^* = \arg\min_\theta \frac{1}{2}||U(\theta) - d||_2^2 + \alpha R(\theta). \tag{2.3}$$

Here, the first term enforces that reconstructions fit the data, whereas the second term is the so-called regularization term. As discussed previously, this regularization term is necessary when dealing with inverse problems, as it prevents a solution from over-fitting the measurement noise. Importantly, by incorporating prior knowledge in the design of R [22,23], we effectively choose preferred solutions and overcome the problem of non-uniqueness. Finally, the parameter $\alpha > 0$ balances both terms and depends on the noise amplitude. Solutions to (2.3) are computed by suitable optimization schemes, for which repeated evaluation of the forward model U will be necessary. Consequently, computing solutions to (2.3) can be highly expensive, if the evaluation of U is expensive. Thus, for nonlinear problems fast converging algorithms, such as Gauss–Newton or related methods [24], are preferred.

Lastly, with the recent rising popularity of data-driven methods, researchers have designed computationally more efficient ways to address the reconstruction problem [25]. Such data-driven approaches are often inspired by the classical reconstruction algorithms discussed above. For instance, one can replace the direct reconstruction operator, or parts of it, with a data-driven component, typically consisting of a neural network [26–28]. Given a set of informative reference data, one can then learn a suitable mapping mimicking (2.2). Alternatively, researchers have investigated the possibility of improving the iterative process to compute solutions to (2.3), by replacing parts in the optimization algorithm with learned components [14,29–32], or entirely building network architectures motivated by the iterative solution process [33,34]. The use of data-driven methods is expanded upon in §7.

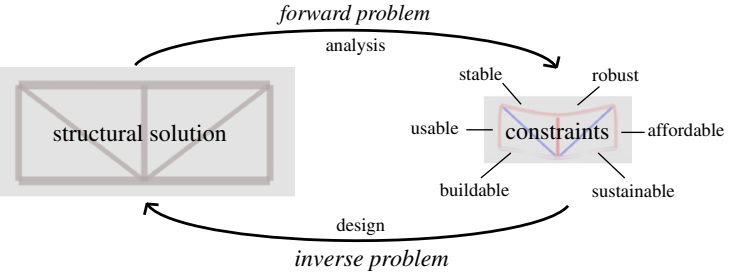

Figure 2. Relationship between structural analysis and design, in which design is the inverse problem of evaluating a suitable structural solution given a set of constraints. Some constraints (such as stability constraints) render themselves more easily to quantitative treatments. (Online version in colour.)

3. Structural design as an inverse problem

(a) Demarcating structural analysis and design

Prior to the Second World War, engineering higher education was originally focused on the art and practice of engineering design [35]. By the 1960s however, owing to the success of science-based ventures such as the Manhattan Project and the rise of government-sponsored research grants that severed the link between academia and industry, engineering science became the main field of research and teaching at universities [36]. This research led to the development of powerful structural analysis techniques, yet also left engineering graduates with a noticeable loss of practical engineering skills [37]. In the 1990s and early 2000s, there was a push to introduce capstone design projects in university engineering degrees to address this shortcoming, the success of which is disputed [38].

There is a broad agreement within the literature that analysis and design are two distinct activities. Structural analysis, which falls into the field of engineering science, is primarily concerned with establishing *knowledge-that* explains the world, whereas design is concerned with *knowledge-how* something works [39]. Design is often characterized as being ill-structured [40], open-ended [41] or even 'wicked' [42], qualities which do not necessarily lend it to science-based research and helps motivate the search for a different paradigm which more adequately addresses its true nature.

One perspective to account for these differences is to recognize structural analysis and structural design as being two different types of problems. Although structural analysis is typically seen as a sub-field of design to validate and justify the adequacy of structural elements [43], we like to advocate the view that structural design is in fact an *inverse problem*, with structural analysis forming the related *forward problem*.

Unlike typical inverse problems such as the one shown in figure 1, where physically measured data (the displacement field) are used to identify the causalities (stiffness properties), in structural design we are dealing with a theoretical construct, or 'theoretically' measured data. These data contain the set of complex design constraints which need to be adhered to, such as ultimate (ULS), serviceability limit states (SLS), sustainability and constructability. From this perspective, structural design can be seen as the process of arriving from a specific set of constraints to a viable structural solution, with analysis being the process of checking if the proposed structural solution adheres to those constraints, as shown in figure 2.

This perspective is evidenced by realizing that the key features of inverse problems, specifically their ill-posed nature as explained in §2, manifest themselves in design. Their shared characteristics include being unstable, non-unique and sometimes unsolvable problems [44]. Note how these qualities were alluded to as 'ill-structured', 'open-ended' and 'wicked' by previous researchers, yet, to the best of our knowledge, this is the first time that literature has attempted to view structural design as an inverse problem.

Table 1. Overview of ill-posed inverse problem features in the context of structural design.

ill-posed inverse problem characteristics	general description	examples in structural design
unstable[a]	small changes in constraints can lead to large changes in the solution space	impact of grid spacing on the selection of appropriate floor options
non-unique	for a given set of constraints, multiple solutions exist	various truss archetypes which can span the same distance
unsolvable	lack of realistic constraining data impedes the search for an adequate solution	current lack of appropriate structural materials for space elevator designs

[a]In reference to the solution space, not structural instability (buckling); see [44].

We suggest that the application of the inverse problem perspective in design gives rise to the idea of a 'design model'. Similar to how an 'analysis model' allows us to evaluate the action effects of a given structural solution, solving the forward problem shown in figure 2, a 'design model' would generate structural solutions which adhere to the given set of user-defined constraints, solving the inverse problem. This perspective sheds light on the characteristics which design problems directly share with other inverse problems, such as the non-uniqueness property. Multiple viable solutions often exist to any given design brief, one example of which are the various truss archetypes for bridge designs to span a similar distance. In order to create a viable design model, it would be necessary to provide some form of regularization, examples of which are provided in §5 in the context of SHM, to effectively encourage design models to choose preferred solutions based on prior knowledge. This could be achieved by constraining the solution space to a sub-set of structural systems, cross-sections or materials based on the specific constraints provided. Other properties of inverse problems which arise in design are shown in table 1 and a comprehensive understanding of the application of the inverse problem perspective warrants further research using specific design examples.

We note that the design problem can be also formulated as an optimal control problem [45], where the optimal design parameters are thought to be found as a minimizer of a penalty function while satisfying the system equations. Whereas the optimal control approach can provide an effective way to solve complicated design problems, it falls short in accounting for uncertainties or inaccuracies in the forward model, and especially the link between measurement and system parameters. We believe that here lies the strength of the inverse problems viewpoint, which offers a rich interpretation and link between the system parameters and measurements given as the forward model. This is promising not only for the optimization task in the design process but also for new ways to approach the modelling of the forward problem.

(b) The link to structural optimization

As explained in §2, inverse problems can effectively be solved iteratively [46]. This process involves making an estimate of the structural solution based on experience and design heuristics (such as simple rules of thumb), checking those estimates through an analysis (forward) model and updating the model if necessary; in other words, this approach is characterized by creating an optimization problem. Some examples of forward-driven optimization models used in structural design include: optimizing the deformed shape of flexible formwork structures to predefined target geometries [47,48], best-fit geometry optimization of thrust networks in the design of shell structures [49] and finding the optimal structural forms for long-span bridges [50], gridshells [51], trusses [52], portal frames [53] and structural sections [54].

A key theme in these research works is that the structural geometry or member proportions are not initially defined, but rather are form-found or discovered in the process, based on the

defined loading, boundary conditions and objectives. Often these discovered structural forms may lead to step change benefits in terms of performance or reduced material usage, as they are unbiased by our preconceived perception of what a 'good' structure is, or by what we currently design and build in the construction industry with standard template solutions. It is also true for many cases that a solution may not even exist, forcing us to accept a closest best fit solution, or it can be that an optimal solution may have multiple candidates by virtue of the structure's static indeterminacy. A common problem with a forward (sometimes brute force) optimization approach, can be lengthy computational times for structural analyses in the objective functions, and the sheer size of the design (and hence optimization) search space, stemming from many wide-ranging input design variables. While fast and globally convergent convex optimization programs can be set up, many practical structural engineering design problems are inherently nonlinear in nature, forcing a slower approach that uses local searches or heuristic methods with no guarantee of a global optimum. This is a current challenge faced in solving inverse problems iteratively with forward models.

(c) Implications of treating structural designs as inverse problems

This inverse problem perspective has various implications. Firstly, it should emphasize that design problems ask a different question from those related to analysis. An analysis model solves the forward problem, and answers questions such as: What is the ULS utilization ratio of a particular beam system for a specific load, with the following specific cross-sections and support conditions? An appropriate design model would ask the reverse: What is the group of cross-sections and support conditions which ensures a utilization ratio of less than 1.0 for this particular beam system to carry this particular load? In this formulation, the magnitude of loading and the utilization ratio serve as the design constraints (both are known 'data'). Whilst engineering science has produced sophisticated analysis models, the research of such 'design models' is lacking in academia.

Secondly, the inverse problem perspective sheds insight on the possibility of using data-driven approaches as opposed to more typical optimization techniques. The rise of machine learning and deep neural networks could be used for the development of such 'design models', which focus on directly identifying a set of structural solutions from a given set of constraints using learned data. Such models could address some of the challenges faced in design due to tight deadlines that force early design decisions, whose full implications might only be realized at the detailed design stage when changes become cost and time prohibitive. This can lead to structural solutions that are difficult to build, have poor sustainability metrics and can be costly to engineer and fabricate. If one instead considers the design process in an inverse manner, rooting firmly first at the end goal, it could be possible to reduce project risk and pick more effective structures by appreciating many solutions to the brief from the onset. This was already alluded to in §2 and is expanded upon in section §7.

Lastly, the ultimate benefit of an inverse problem perspective is that it helps to clearly distinguish between analysis and design procedures and provides academia with an adequate framework to contextualize *design model* research. Engineering academia has been dominated by the engineering science perspective [55], predominantly choosing to research and teach forward problems. One of the uncomfortable implications of this view is that engineers from over 150 years ago, who trained primarily in the art and practice of engineering design, may in fact have been better 'inverse-problem solvers' than academics and graduating engineers of today (who are stronger in solving the well-structured forward problems) [56]. This might help swing the pendulum away from focusing exclusively on forward models (analysis) towards a more stable equilibrium with inverse models (design) by acknowledging the existence of these two related, albeit distinctively different, types of problems. The use of inverse problem and inverse analysis in a related field to structural design, notably blast engineering, is discussed next.

4. Extreme loads on structures

(a) Blast loading and inverse analysis

High-rate dynamic loads can arise from events such as earthquakes, wind, tidal waves, impacts and accidental or malicious explosions. Here, the imparted load may be comparable to or several times larger than the strength of the material it is acting on, it can be applied and removed in sub-second durations and it is often highly localized. Accordingly, the notion of static structural design according to a pre-determined distribution of stresses and strains may not be appropriate, and instead the designer must consider energy balance, nonlinear analyses and deformation modes for which there is no equivalent static counterpart.

Blast loading is undoubtedly one of the most aggressive forms of dynamic loading. When an explosive detonates it undergoes a violent and self-perpetuating exothermic chemical reaction, releasing energy through the breaking of inter-molecular bonds during oxidation [57]. The explosive material is converted into a high-pressure (10–30 GPa), high-temperature (3000–4000°C) gas which violently expands, displacing the surrounding air at supersonic velocities (6–8 km s^{-1}). This displacement causes a shock wave to form in the air, termed a blast wave, which eventually detaches from the expanding detonation product 'fireball' and continues to propagate into the surrounding air, decreasing in pressure and density as it expands.

When a blast wave encounters an obstacle some distance from the source it will impart momentum as the air is momentarily (either fully or partially, depending on the compliance of the obstacle) brought to rest at the air/obstacle interface. Prediction of blast even in the most simple settings is a considerable challenge to the scientific community. This becomes an increasingly complex and multi-faceted problem when considering issues such as: obstacle orientation; proximity of the obstacle to the source and additional momentum transfer from fireball impingement; secondary combustion effects either at the air/obstacle interface or in late time owing to partial or full confinement of the explosive products; and the presence of mitigating or blast-enhancing materials (soil, reactive munitions, etc.).

Real-world blast events are highly uncertain, and the need for inverse analysis is clear: it is very rare that the exact size, shape, composition and location of an explosive device is known *a priori*. Instead, information relating to the *cause* of an explosion should be estimated, within reason, from the more readily observed *effects*, i.e. the magnitude and severity of structural damage to surrounding buildings and cratering of the ground surface. While inverse analysis is well established for practical post-event assessment of explosions—and has been used to determine the size/location of blast events through forensic investigation of social media videos [58] or numerical modelling correlating structural damage [59,60]—the use of inverse modelling in an academic context is yet to be exploited fully. In the former, order-of-magnitude estimates are typically deemed sufficient, whereas the latter requires repeatable, precise measurements and high levels of experimental control.

The lack of robust yet high-fidelity experimental techniques has stifled academic research into close-in blast for some time. Close-in blast is typically defined as the region within approximately 20 radii from the charge centre, where loading in this region is characterized by a near-instantaneous rise to peak pressure of the order of 100–1000 MPa, followed by a rapid decay to ambient conditions typically occurring in sub-milliseconds. The subsequent structural response may reach a peak value of the order of 10–100 mm and, while this may occur orders of magnitude slower than load application, deformation cycles are still generally within millisecond durations.

Recently, two notable advancements have been made in experimental characterization of close-in blast and structural response. In the first of these, researchers at the University of Sheffield (UoS), UK, developed a large-scale apparatus for the spatial and temporal measurement of blast pressures from close-in explosions [61,62]. In the second, researchers at the University of Cape Town (UCT), South Africa, adapted the well-known digital image correlation (DIC) technique to measure the transient response of the rear face of blast-loaded plates [63]. These two techniques were combined in a recent study [64,65] where, for the first time, detailed loading maps and

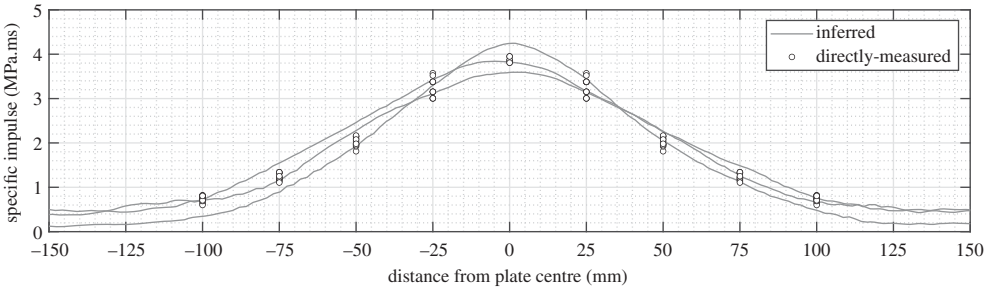

Figure 3. Directly measured (UoS) and inferred (UCT) specific impulse distributions from studies of blast loading and plate deformation following detonation of spherical explosives, expressed at 100 g (UoS) scale; after [64].

temporal structural response profiles were developed independently, in a single-blind study, for identical (scaled) experimental set-ups.

(b) Proof-of-concept experimental studies

Of the experiments performed in [64], 12 are relevant to the notion of inverse analysis of blast loading and structural response, and will be discussed here. Six tests were performed with spherical explosive charges; three at UoS measuring blast loading and three at UCT measuring structural response. In the UoS spherical tests, 100 g PE4 charges were located at 55.4 mm clear distance from the centre of a nominally rigid target, on which the reflected blast pressures were measured. In the UCT spherical charge tests, 50 g PE4 charges were located at 44.0 mm clear stand-off distance from the centre of the flexible target plates: 300 mm diameter, 3 mm thick, Domex 355MC steel plates, fully clamped around the periphery. The plate response was filmed using a pair of stereo high-speed video cameras and DIC was used to determine the transient plate response. The two test series can be expressed at the same scale using well-known geometric/cube-root scaling laws. Here, it is assumed that the flexible targets deform on time scales that are orders of magnitude longer than the loading application, and therefore differences between the loads imparted to the rigid and flexible plates are negligible.

Specific impulse is given as the integral of pressure with respect to time. Numerical integration of the UoS pressure histories (at various distances from the centre of the plate) yields *directly measured* specific impulse distributions. The first few frames of the UCT tests were used to determine initial velocity distributions of the plate, from which the imparted specific impulse could be *inferred* through localized conservation of momentum: $i(x) = v(x)\rho t$, where i is the specific impulse, x is the distance from the plate centre, v is the out-of-plane velocity of the plate, ρ is the density (7830 kg m^{-3} for Domex 355MC) and t is the plate thickness.

The results for the spherical tests are shown in figure 3. The full-field inferred specific impulse distributions are in close agreement with the discrete, directly measured values, and both measurements form a tight banding in an approximate Gaussian distribution [66]. Not only does this indicate a high level of test-to-test repeatability for each method, but also demonstrates that the two methods are measuring the same underlying phenomena, albeit in entirely different ways. Thus, it can be said that an imparted impulse will result in an initial velocity uptake which is directly proportional, and therefore measurement of one allows for the other to be determined. This proves the concept of using plate deformation under blast loads in an inverse approach—namely that from knowledge of plate deformation one may be able to determine the imparted load—and provides physical verification of the inverse approach developed by [67,68].

In addition to the spherical charge tests, six tests were performed in [64] using squat cylinders (height:diameter of 1:3). Such charges are known to produce a more concentrated load, with the fireball propagating at higher velocities along the axis of the charge [69]. This accelerates the growth and emergence of surface instabilities [70], which gives rise to a more variable loading

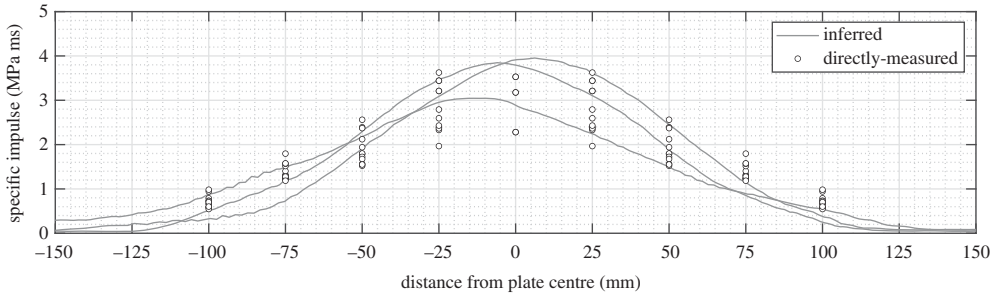

Figure 4. Directly measured (UoS) and inferred (UCT) specific impulse distributions from studies of blast loading and plate deformation following detonation of cylindrical explosives, expressed at 78 g (UoS) scale; after [64].

distribution [71]. A key research question in this study was: Will a more variable loading result in a more variable structural response? In the UoS cylindrical tests 78 g PE4 charges were located at 168.0 mm clear distance from the centre of the target, and in the UCT cylindrical tests 50 g PE4 charges were located at 145.0 mm clear distance from the centre of the target. Again, specific impulse distributions were both directly measured and inferred from the plate response, respectively, and the experiments were expressed at the same scale using common scaling laws.

The results for the cylindrical tests are shown in figure 4. While the two methods again show good agreement, the results can be seen to form a much wider spread. In contrast to the spherical tests, where peak specific impulse was seen to consistently act in the plate centre for all tests, here the peak value is often up to 25 mm from the plate centre (approximately equal to the charge radius), in both the directly measured and inferred values. The inferred values are generally bounded by the directly measured values, which suggests that this spread is indeed a genuine feature caused by application of a more variable load.

(c) Outlook

The aforementioned studies [64,65] have provided a firm physical basis for inverse analysis in the context of extreme loading and structural response. The results have clear implications for the future of research in this area. Namely, it has been demonstrated that not only can inverse analysis provide excellent predictions of blast loading in repeatable, well-controlled situations (as with the spherical tests in [64]), but also structural response measurements are potentially sensitive enough to detect localized variations in loading (as with the cylindrical tests in [64]). This is particular important in situations where a highly variable loading might be expected (e.g. from explosives buried in well-graded soils [72]), but statistical variations cannot be determined in a robust sense when using direct measurements (note the discrete nature of the direct measurements in this study, compared with the effectively continuous nature of the inferred measurements). This technique may permit, through inverse methods, fundamental scientific studies of complex mechanisms governing blast loading following close-in detonation of explosive charges in situations where previous research has not yet been possible.

5. Structural health monitoring

(a) Background on inverse methods in SHM

Unlike the fields of structural design or blast engineering, it is well known that inverse problems are deeply connected to SHM. In fact, computerized damage detection can generally be recognized as either a pattern recognition or inverse problem [10,73,74], where unknown or uncertain parameters (causalities) are estimated via quasi-static or dynamic structural response data. Among the numerous inversion-based approaches, FEM updating methodologies are

among the most pervasive [75–78]. Much of the noted popularity is owed to the flexibility of the FEM for comparing modal parameters with an undamaged state and in compensating model errors.

Meanwhile, analytical [79], wavelet [80], fractal [81], fuzzy system [82], Kalman filter [83], chaotic interrogation [84], shape function [85] and particle filtering [86] approaches, among many others, have proven successful in uncertain inverse parameter identification applications within SHM. Broadly speaking, inverse SHM approaches can be grouped as either deterministic or probabilistic [87]—which is also generally the case in classical inverse problems [13]. In the latter case, estimation of uncertain SHM parameters takes the form of a probabilistic term; for example, a value with an associated certainty, a probability itself, etc.

Irrespective of the computational approach used in damage detection, two key realizations affect the efficacy of inversion methodologies: (i) a baseline is generally needed to detect/quantify damage [88] and (ii) the presence of damage inherently influences the linearity of structural behaviour [89]. In addressing (i), reference-free or baseline-free frameworks have been introduced [90–93] via the introduction of either assumptions on the reference state, implementation of prior physics knowledge or probabilistic regimes. On the other hand, nonlinearity in the structural response can either act as a corrupting entity when linear forward models are used (e.g. unacceptable forward model error) or be used as an advantage when properly leveraged. Regarding the latter, as noted in [89], methods based on nonlinear indicators, dynamical systems theories and nonlinear systems identification approaches can be used to aid or enrich the damage identification process; such a conclusion can also be extended to the pure usage of inverse approaches in damage detection.

In the past 30 years, implementation of inversion-based damage detection methods in SHM has steadily increased. This is the result of the increase in both inverse problems know-how and computational resources. Yet, since the emergence of contemporary machine learning, the ability to solve problems deemed previously intractable has exponentially increased opportunities in this area. For example, in many cases, forward models may not be available or are too computationally expensive, sufficient nonlinearity may exist to effectively model the desired physics, errors in highly reduced models may be excessive, the ability to compute model gradients may be overly expensive, etc. Moreover, the ability of classification networks to readily classify important variables such as the probability and/or severity of damage from structural data is intuitively appealing and pragmatically useful. In the following, we will provide contemporary examples highlighting the use of both classical and machine learning-based SHM inverse approaches.

(b) Static inverse problems in SHM

Incorporation of discrete static (or quasi-static) data measured from structures into SHM frameworks is well established. For example, a number of sources, including corrosion, relative humidity, fibre-optic, topography, laser, potentiometer, strain gauge, electrical and thermal sources, have been successfully integrated into long-term condition monitoring protocols [94]. The richness of spatial–temporal data obtained from these sources lends itself well for use in inversion-based SHM, i.e. given a set or sets of static SHM data, use an inverse methodology in capturing (potential) damage. This is true in cases where numerical models are available for the problem physics and when they are not (e.g. learned models can act as surrogates when physics-based models are unavailable).

The sheer volume of literature available reporting the successful use of static inversion methods in SHM is formidable. However, roughly speaking, static inverse methodologies have been implemented within three areas: (i) point sensing, (ii) area sensing, and (iii) volumetric sensing. Holistically, it can be difficult to distinguish between each of these areas; for example, when lower dimensional measurements are extrapolated to characterize damage in area or volume targets [95,96]. One such example is DIC, where the displacement field at discrete points on a structure is inversely computed via pixel movement and then extrapolated (interpolated) to a full field, whereby the quality of the computed field is highly dependent on the quality

of the contrasting area speckle pattern [97]. Similarly, one may consider the distinguishing of static measurement dimensionality as a local–global phenomenon where discrete local changes contribute to the analysis of the global structural system [95]. Lastly, to complicate matters even more, the use of discrete measurements can yield two- (2D) or three-dimensional (3D) information—as in the case of penetrative electrical measurements, where currents diffuse through the entirety of a body [98].

Fortunately these, perhaps philosophical, realizations are often washed out via the nature of inversion methodologies themselves. Pragmatically, at least in the context of SHM, the solution to static inverse problems generally requires a model, either physics based or learned. As such, the amalgamation or assimilation of data and solution dimensionality is often simply a matter of discretization or model generation. In a similar vein, when static inverse problems are ill-posed, solutions generated using lower dimensional data are regularized/biased using prior models consistent with the solution dimension.

Many examples are available in the literature illustrating the efficacy of static inversion methodologies for applications in a suite of SHM implementations. For example, the use of displacement measurements for capturing SHM causalities in various structural geometries was reported in [99–101]. Of note, the specific applications using displacement fields to reconstruct elastic and elasto-plastic properties (and corresponding damage characteristics) have been the source of significant research [102–117]. In the pervasive case where displacement/strain measurements are discretely measured from strain gauges/fibre-optics, inverse methodologies have also been fruitfully employed for damage characterization, pressure and strain mapping, and shape sensing [118–129]. Perhaps one measure illustrating the success of such inverse approaches is highlighted by the recent interest in optimizing the related sensing schemes [118,130–132].

In the past decades, the emergence of electrical inverse methods has also proven a viable approach to static condition monitoring [133,134]. This family of inversion-based modalities generally uses three different data sources, including capacitative, direct current and alternating current-based measurements. Capacitative sensing is perhaps the newest of these approaches to sensing, where SHM causalities can be inversely computed using smart bricks [135], area sensors [136–139] and electrical capacitance tomography [140,141]. On the other hand, owing to its established history in medical and geophysical applications, electrical impedance tomography (EIT, or electrical resistance tomography, ERT) is becoming a well-established approach to damage detection, reconstruction and localization, especially in concrete applications. For these, EIT presently manifests via two approaches, reconstructing conductivity maps using boundary voltages measured from area-sensing skins [142,143] or directly imaging a 3D cementitous body [144]. Representative 2D EIT reconstructions are provided in figure 5 using a machine-learned approach (direct reconstruction) for imaging flexural and shear cracks in concrete elements. To this end, EIT has also been used for characterizing area corrosion [143] and localizing area temperature variations [145].

In summary of this sub-section, it is clear that the use of inverse methodologies in static SHM applications is pervasive. Meanwhile, a number of inversion-based modalities are still emerging—or are yet to emerge. Indeed, given the number of potential static data sources available at present, there exist substantial opportunities to investigate or formulate new inversion-based modalities. In the light that some physical models for various underlying physics remain unavailable (either in open source or in general), the use of learned models may bridge this gap. Lastly, there currently exist tremendous opportunities in the areas of data fusion and joint imaging, which remain predominately unexplored in the area of static inversion-based SHM [146].

(c) Dynamical inverse problems in SHM

The use of dynamical data for monitoring the health and condition of structures is well established [147]. For this, a number of data sources are available, for example discrete acceleration,

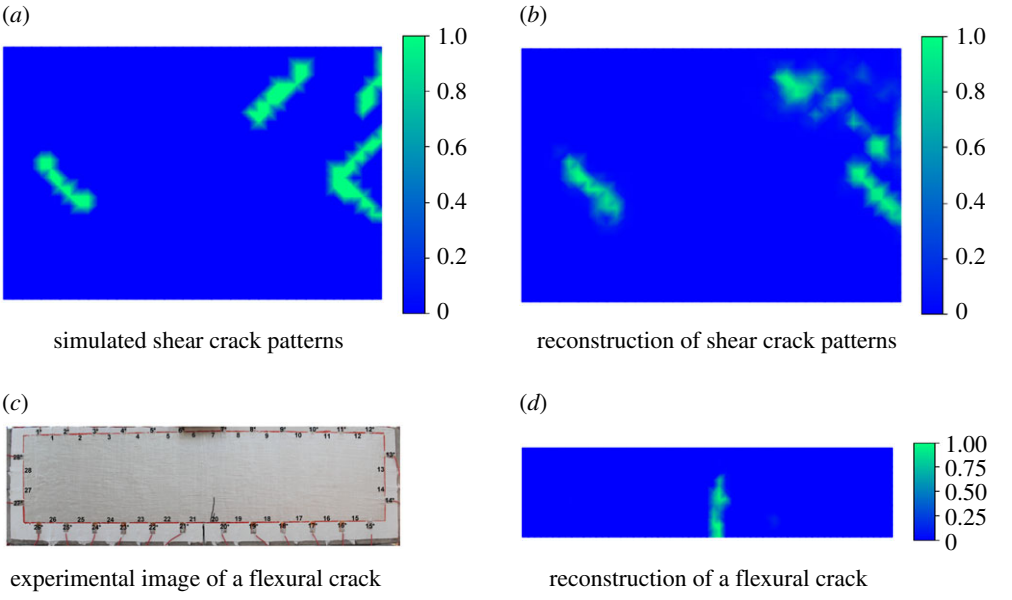

Figure 5. Reconstructions (right column) report probabilistic predictions of local flexural and shear cracking in concrete elements. The colour bars represent the probability of cracks at nodal locations: (*a*) simulated shear cracking pattern, (*b*) probabilistic prediction of the shear crack pattern using a convolutional neural network, (*c*) photo of a flexural crack in an area-sensing skin and (*d*) probabilistic prediction of the flexural crack using a feedforward neural network. (Online version in colour.)

strain, displacement measurements and, recently, coupled electromechanical impedance via piezoelectric transducers [148,149]. In the case of typical civil infrastructure [150], the ability to actively excite monitored structures is pragmatically challenging owing to the extreme magnitude of the excitation required to attain a distinguishable response. For this reason, ambient monitoring methodologies have gained significant popularity in recent years [151–153]. Irrespective of the dynamical monitoring approach used, extracting dynamical structural properties of interest can be viewed as an ill-posed inverse problem [154]. The ill-posedness of such problems results from a number of actualities, not limited to uncertainties in environmental conditions (wind, temperature, ground conditions, humidity, etc.), traffic, measurement noise, the discrete nature of measurements, material characteristics and numerical modelling error.

One of the most pervasive frameworks used in solving dynamical inverse problems is model updating, which generally aims to match a physics-based model (such as a representative finite-element model) to measured dynamical data [73,89], commonly using a form of modal analysis [155–157]. The physics-based techniques are particularly efficient in providing higher accuracy when testing is restricted. It is often the case that reconstructing the dynamical SHM properties of interest proves difficult, requiring an innovative approach; some proposed frameworks have included advanced optimization protocols [158] and mode decomposition/superposition [159]. Alternatively, the use of phase space [160], state space [161], singular value decomposition, the λ-curves method [162,163] and auto-regressive [164,165], Gaussian process [166] and Bayesian/stochastic approaches [167–170] has proven successful. As noted in the previous sub-section, one metric for assessing the progress in this field is the number of works aiming to optimize sensing information, for example in [132,171–178].

In the past 20 years, guided wave-based modalities have emerged as a viable approach to dynamical inversion-based SHM [179–186]. Common physical manifestations of guided waves include Lamb waves (propagating through thin shell and plate structures) [187], Rayleigh waves (surface waves) [188] and shear waves. Generally speaking, SHM systems consist of transducer systems used for actuation and measurement accompanied by an inversion algorithm

aiming to reconstruct SHM causalities of interest. Owing to a number of numerical challenges, conventional solutions to related inverse-guided wave problems are generally not feasible [183]. Consequentially, alternative methodologies have been proposed, including, for example, inverse filtering [189], reverse time migration [190,191] and Bayesian/probabilistic [192,193], among emerging inversion approaches.

While the use of dynamical inversion-based techniques is well established in conventional monitoring, in some areas (such as guided wave monitoring) it remains in the early stages of development and affords numerous research opportunities. It is worth mentioning that with the advent of modern machine learning methods, we can only anticipate significant advances in forthcoming years as trained networks are now capable of addressing key SHM challenges related to, for example, model error estimation/correction [194] and reducing computational demands associated with many SHM facets [195,196].

(d) Computer vision inverse problems in SHM

In addition to the discussed static and dynamic inverse problems in SHM, computer vision-based SHM methods have become an emerging field in inverse engineering problems in approximately the past decade. Relying on digital images and videos, vision-based SHM techniques enable affordable and rapid structural prognosis. The concept of vision-based inverse problems is straightforward: visual information from the external surfaces of structures is captured through digital cameras, serving as input data for computer vision algorithms in detecting, localizing and quantifying structural damage in a variety of contexts.

Computer vision-based inverse problems can be either static or dynamic in nature. In dynamical environments, a digital camera is treated as a vision sensor measuring dynamic structural responses. Instead of directly capturing the structural vibration through contact-based sensors (e.g. accelerometers), vision-based algorithms can track structural responses through a video stream. For example, in [197], researchers applied a video feature tracking technique to measure the pixel movements of a steel girder in a football stadium under a service load using a consumer-grade digital camera. These movements were then converted into displacements using a scaling factor. Similar efforts have been reported in [198,199]. Furthermore, through the use of cameras as displacement sensors, other key structural features, such as natural frequencies/mode shapes [200,201], beam influence lines [202] and bridge cable loads [203], have been be estimated.

In addition to tracking the surface motion, computer vision algorithms can offer rapid and reliable inspections against structural damage such as cracks [204], concrete spalling [205], steel corrosion [206] and other structural deterioration [207]. To make this viable, researchers develop vision-based algorithms to scan and extract damage-induced visual features either across the entire image scene or within a small predefined image patch (e.g. region of interest) that is prone to structural deterioration. In general, the image-based damage extraction techniques can be categorized as: (i) machine or deep learning-based methods and (ii) non-learning based methods.

The idea of machine or deep learning-based (computer vision) methods is to train a damage detection classifier through an image dataset with pre-labelled structural damage. Then, the classifier is applied in characterizing structural damage from newly captured images. Some of the successful applications include detection of concrete cracks [208,209] and spalling [205], steel cracks [210], bolt loosening [211,212], steel surface defects [205], pavement cracks [207] and complex situations where multiple damage types exist [213]. By contrast, non-learning-based methods can directly pick up image features caused by structural damage, and hence do not require any prior knowledge in training the classifier. For instance, fatigue cracks in steel bridges can be identified through crack breathing behaviour [214]. Also, loosened bolts in steel connections can be quantified by extracting the differential features provoked by bolt head rotations [215]. Figure 6 illustrates an example by comparing two images of a steel connection at different inspection periods to extract the differential features provoked by the loosened bolts.

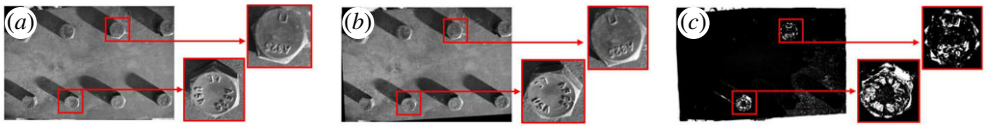

Figure 6. An example of vision-based bolt-loosening detection where (*a*) and (*b*) are images of a bolted connection taken at different inspection periods. Two loosened steel bolts are shown in the blow-up figures with counterclockwise rotations in their bolt heads. Using a series of image-processing techniques, the differential features caused by the bolt loosening can be identified in (*c*). Detailed discussion can be found in [215]. (Online version in colour.)

Computer vision-based methods can be extended for damage detection and pattern recognition in full-scale civil structures. Using the platform of unmanned aerial vehicles (UAVs), the on-board UAV camera can rapidly scan the structure, including the locations that are challenging to be accessed by traditional contact-based sensors. For example, researchers in [216,217] applied UAVs and vision algorithms to leverage effective approaches for post-earthquake building safety inspections. Similar efforts have been reported for inspecting dams [218,219], tunnels [220] and railways [221]. Other researchers adopted satellite images to examine damage status over a larger scope of work (i.e. multiple buildings at the community level) after natural disasters such as flood, earthquake, volcanic eruption, hurricane and wildfire [222,223].

UAV platforms are also capable of collecting a large volume of images of civil structures under different camera angles through automated route planning. Such an advantage can be further enhanced by a computer vision workflow, termed photogrammetry, for the purpose of reconstructing the 3D model of the structure. Relying on structure-from-motion with multi-view stereo (SfM-MVS) algorithms [224], the photogrammetry technique can create a 3D structure model (e.g. a 3D point cloud) based on 2D images. Photogrammetry leverages several potentials in inverse SHM problems. For instance, in recent work, [225] created a dense point cloud of a building in a construction site based on UAV images. Then the point cloud was integrated with a building information model (BIM) to label the structural components in the original UAV images. In [226], the researchers used the dense point cloud to assist the creation of a finite-element model of a masonry bridge. The authors argued that the benefit of using the point cloud was twofold: the point cloud depicted the accurate geometric information of the bridge and offered the results of bridge crack distribution. In [227], researchers leveraged the photogrammetry workflow to find concrete cracks and spalling of a highway bridge. Lastly, in the context of the 2021 Hernando de Soto Bridge incident [228], where a large crack was discovered in a 'fracture critical' element by a private engineering firm—yet, was previously identified approximately 2 years earlier by a local operating a commercially available drone—the use of coupled UAV/computer vision approaches to SHM may be more valuable than ever.

(e) Digital twins and outlook

As this section has illustrated, the use of inverse methodologies in SHM is both well established and an area of active development. With the rapid digital transformation of structural assessment and infrastructure asset management, the emergence of numerous digitally inspired technologies will play a key role in the future trajectory of inverse problems in SHM. At the forefront, *digital twins* have been the source of increasing research and industrial interest in recent years [229]. While the scope of digital twins' applications spans beyond SHM alone, its basic aim is to provide information on the current or future state of an asset by combining real-time data, and a physical/data-driven model offers many potential avenues for engagement with the inverse problems community. Nonetheless, in specifically considering a classical SHM application, such as damage localization [230], developments stemming from the inverse community, including, for example, state estimation [231–233], uncertainty/model error approximation/compensation [194,234,235], regularization [236] and model reduction [237], have excellent potential for enriching or enhancing digital twin frameworks.

As a whole, the future outlook for the integration and advancement of inverse methodologies in SHM is very bright. Indeed in the past 20 years, we have seen an exponential increase in high-performance computing and graphical processing unit development and assimilation into modern civil and mechanical engineering applications [238,239]. Coupled with powerful inverse frameworks for large-scale problems (e.g. Krylov solvers [240] and distributed computing [241]) and machine learning [242], we can only expect (i) a steady increase in the breadth of the inverse problems that the SHM community is able to address and (ii) an evolution in innovative inversion-based approaches to solving increasingly challenging SHM problems.

6. Smart materials and structures

Smart, *self-sensing* materials have received immense attention in recent decades [243–245]. A material is said to be self-sensing if it exhibits a property change in response to external stimuli. These materials are able to intrinsically report on their health or condition in a spatially continuous manner and with less hardware/instrumentation burden than traditional point-based sensing technologies (e.g. strain gauges, piezoelectric patches, accelerometers, etc.). In structural engineering, external stimuli are often mechanical effects such as deformation, damage or loads. Hence, integrating smart materials into next-generation structures may allow for unprecedented health monitoring and diagnostics. A discussion on smart materials in structural contexts may therefore also be considered as a subset of the preceding discussion on SHM (see §5). Nonetheless, we will treat it as a distinct topic in the forthcoming sections owing to its unique inverse problems.

Although self-sensing is an umbrella term encompassing many different physical effects, the *piezoresistive effect* has perhaps received the most attention to date (see recent reviews [243,246,247]). Piezoresistive materials are so-named because they exhibit a change in electrical conductivity (or its inverse, resistivity) upon deformation. This means that every point of the material is capable of relaying information on its mechanical state. Damage such as voids, ruptures or fractures can also be detected since the removal of material represents a conductivity loss. But spatially continuous piezoresistive sensing presents two challenges of relevance to inverse problems: (i) it is not practical to instrument electrodes at every point on a structure, which means that it is necessary to deduce conductivity distributions from a finite set of measurements, and (ii) even if we could recover a spatially continuous mapping of the conductivity, electrical properties are of little consequence to the structural engineer. We would much rather know the underlying mechanics that give rise to an observed conductivity distribution. We will address both of these inverse problems. First, however, a brief summary of the physics and piezoresistive modelling approaches is given. It will be seen later that modelling techniques are essential to solving inverse problem (ii) above.

(a) Piezoresistive nanocomposites

Many materials intrinsically exhibit piezoresistive properties. For example, carbon fibre-reinforced polymers (CFRPs) are well known to change conductivity when loaded elastically [248,249]. Here, however, we will instead focus on materials that have been *engineered* to be self-sensing; that is, an additional constituent has been added to the material system without which it does not exhibit piezoresistivity. This is most commonly done by adding a conductive phase to a non-conductive matrix such as polymers (including structural polymers such as epoxy vinyl ester [250], polymeric thin films for use as sensing skins [251], laser-induced graphene inter-layers in continuous fibre composites [252,253] and even polymer binders in energetic materials [254,255]), cements [256] or ceramics [257]. Electrical transport is then a consequence of percolation—the composite conducts electricity when enough fillers have been added to form an electrically connected network. Because the percolation threshold decreases with aspect ratio, fillers with ultra-high aspect ratios such as carbon nanotubes (CNTs) are popular. There are considerable challenges associated with manufacturing CNT-based nanocomposites such as achieving good dispersion—ultra-small fillers such as CNTs have a tendency to agglomerate, which can degrade

the mechanical properties of the composite. But manufacturing is outside the scope of this manuscript and is well covered elsewhere [258,259].

Considerable effort has also been devoted to the development of piezoresistivity models—computational and/or analytical means of predicting how conductivity changes for a prescribed strain. These efforts can be broadly categorized as (i) equivalent resistor network models [260–262], (ii) computational micro-mechanics models [254,263–265], or (iii) homogenized macroscale models [266–268]. In (i) equivalent resistor network models, high aspect ratio fillers such as CNTs are represented as either straight or wavy/curved sticks in a micro-domain [260–262]. These sticks are discretized into resistors based on the length, diameter and conductivity of the fillers, and junctions between nearby fillers are discretized into resistor elements based on the equivalent resistance felt by an inter-filler tunnelling electron [269]. The conductivity of the nanocomposite can then be calculated from the overall resistance of the discretized nanofiller network and the dimensions of the micro-domain. For a given deformation of the micro-domain, the translation and rotation of the fillers can be calculated by treating them as rigid inclusions [270]. Post deformation, the conductivity of the micro-domain is recalculated, thereby allowing piezoresistive properties to be predicted.

Second, (ii) computational micro-mechanics models use computational means to simulate both phases of the composite—the non-conductive matrix and the conductive fillers [254,263–265]. Because of this, and unlike equivalent resistor network models, computational micro-mechanics models can incorporate nuanced effects such as nanofiller-to-matrix debonding, nanofiller deformation, etc. A limitation of this approach is computational expense owing to individual nanofillers and the enveloping matrix being explicitly simulated. It is therefore difficult to scale these models to structural levels.

And third, (iii) homogenized macroscale models describe the conductivity of the nanocomposite as an analytical function of the strain state without simulating individual fillers. Rather, conductivity/resistivity strain are coupled through analytical functions based on excluded volume theory [267] or via 'constitutive' tensors (note that these are not proper constitutive relations because conductivity and strain are not energy complements) [268,271,272]. This approach is therefore less computationally expensive than equivalent resistor network and computational micro-mechanics models. Importantly, homogenized approaches can be readily integrated with structural analysis tools such as the FEM, thereby allowing for macroscale piezoresistive analyses. As will be discussed in §6c, this allows for strain recovery via piezoresistive inversion. Despite these advantages, analytical models suffer from having to make assumptions regarding average inter-filler spacing, average orientation of nanofillers and the need for calibration data.

(b) Conductivity imaging via EIT/ERT

As discussed in §5b, conductivity imaging modalities such as EIT (or DC resistivity imaging via ERT) have been explored for health monitoring in structural materials [247]. EIT is a natural complement for piezoresistive materials because it allows for the spatial localization of damage and the *mapping of deformation and strain.* There are several factors that make the EIT interesting to pair with self-sensing materials: (i) This combination allows for sub-surface strain imaging. That is, a myriad of techniques exist for monitoring surface strains such as strain gauges, DIC, holographic methods, etc. Tools for studying sub-surface strains, however, are much more limited, often require ionizing radiation and can be costly (e.g. volumetric strains via X-ray digital volume correlation [273]). (ii) Traditional 'limitations' of EIT can be strengths in structural applications. For example, the simplest implementation of EIT favours spatially smooth solutions. This is obviously undesirable when imaging discontinuous features with distinct boundaries such as organs in a living body. Strain fields, however, are often smoothly varying, thereby playing to EIT's strengths. And (iii), because piezoresistive materials are engineered, we can leverage our knowledge of their piezoresistive response to build bounds into the EIT inverse problem. Two examples of strain imaging via EIT in self-sensing polymeric composites are shown in figure 7.

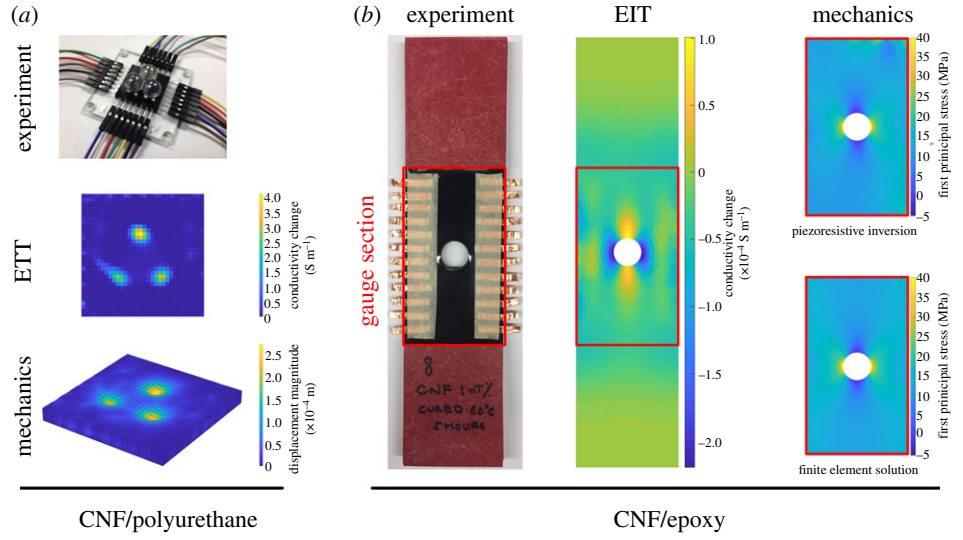

Figure 7. Examples of EIT and piezoresistive inversion applied to self-sensing nanocomposites. (*a*) A soft carbon nanofibre/polyurethane (CNF/PU) is deformed by rigid, non-conductive indentors [274]. EIT is then used to image the deformation-induced conductivity changes, and piezoresistive inversion is used to recover the displacement field (multiplied by a factor of 5 for ease of visibility). (*b*) A hard CNF/epoxy is loaded in tension with a stress raiser at its centre [275]. EIT is again used to image the conductivity change. Lastly, piezoresistive inversion is used to recover the underlying displacement field. With knowledge of the material's elastic properties, strains and stresses can be spatially mapped. The first principal stress of the guage section is shown here along with comparison with a traditional FEM solution for validation. (Online version in colour.)

Both examples leverage knowledge of conductivity change bounds to build constraints into the solution space. Beyond these advantages for structural imaging, the pairing of EIT/ERT with self-sensing materials may also have keen, as-of-yet unrealized potential for extreme loading (particularly self-sensing energetic materials [254,255]). That is, it may be illuminating to image energetic materials as they detonate. However, most prevailing imaging modalities do not have the temporal resolution to capture these fleeting moments and require hardware that is too expensive to risk damaging it. EIT, on the other hand, can have ultra-high temporal resolution (of the order of hundreds of microseconds for optimized systems [276]) and uses only low-cost hardware (i.e. sacrificing the hardware during a detonation is of virtually no financial consequence). Thus, there may be much exciting potential for overlap between smart materials + EIT and extreme loading as described in §4.

There have been many studies on the topic of EIT and piezoresistive materials. A few representative examples are summarized in this paper, but interested readers are directed to a recent review for a more in-depth discussion [247]. Some of the first work in this area made use of self-sensing nanocomposite *sensing skins* produced by a layer-by-layer fabrication technique [251,277]. These skins were applied to substrates, and EIT was then used to identify and spatially localize deleterious effects including mechanical etching, pH exposure, impact damage and residual strains from impacts. Further on the topic of polymer-based composites, thin pressure sensors were produced by embedding a non-woven textile modified with CNTs into a soft elastomer. EIT was then employed to visualize various pressure distributions including non-uniform distributions [278]. EIT was also recently applied for damage detection in a ceramic-based composite that was modified with micrometre-sized waste-iron particles [279]. And as a final representative example, self-sensing cement composites have been produced by spray-depositing a CNT-modified latex on the aggregate phase. EIT was then successfully used to localize various damages in the material [280].

(c) Piezoresistive inversion

Even though solving the EIT inverse problem allows for the spatially continuous visualization of mechanical effects in these materials, this poses an obvious problem—structural engineers are generally not interested in conductivity. They would much rather know the spatially varying components of the strain tensor, stress tensor or precise damage characteristics since these factors drive structural analyses and health assessments. Recalling also that various macroscale piezoresistivity models exist as described in §6a, we can formulate another inverse problem as follows: For a given EIT conductivity distribution (or, more directly, for a given set of EIT boundary data) and with an accurate model of conductivity–strain or conductivity–amage coupling for a particular material, can the precise mechanics of the system be recovered?

Both of these piezoresistive inversion problems—strain recovery and damage recovery—are challenging. The former is challenging because, under ideal circumstances, we seek six components (in three dimensions) of a strain tensor from a scalar conductivity field. Prospects can be improved somewhat by instead seeking the displacement field (i.e. three unknowns in three dimensions) from the conductivity data and making use of reasonable assumptions (e.g. plane strain and plane stress) where applicable, but the displacements-from-conductivity inverse problem is nonetheless under-determined. The challenge is exacerbated by the fact that circumstances are never truly ideal; conductivity and conductivity changes are not exactly isotropic, and EIT cannot image individual components of a conductivity tensor. Even for the case of damage imaging, an accurate model of material breakage-induced conductivity change is needed. For simple nanofiller/matrix phase nanocomposites (i.e. without reinforcing fibre), material breakage can be treated as a cessation of conductivity. For more complicated material systems such as nanofiller-modified continuous fibre composites, however, material breakage-induced conductivity changes must account for factors such as anisotropy and residual post-damage conductivity due to inter-lamina contact. And even if a suitable damage model is developed, the inverse solver needs to be capable of reproducing potentially complex damage shapes that are not readily amenable to parameterization. Both strain and damage recovery are additionally hampered by the fact that EIT does not produce accurate conductivity distributions in an absolute sense or a spatial sense.

Despite these challenges, the piezoresistive inversion problem has received some attention. An initial effort used an analytical inversion framework predicated on iteratively minimizing the l_2-norm of an error vector between a predicted and observed conductivity distribution [281]. Although this work was entirely computational and limited to simple deformations and infinitesimal strains, it nonetheless demonstrated that piezoresistive inversion was possible. The next work in this area used EIT to image strain-induced conductivity changes in a carbon nanofibre (CNF)-modified polyurethane (PU) composite [274]. Three marbles (i.e. comparatively rigid non-conductive indentors) were pushed into the CNF/PU as EIT measurements were taken. A similar analytical approach was used to reproduce the displacement field. Two important factors differentiated this study—experimental validation of piezoresistive inversion and successful application to materials undergoing finite strains. Later works looked at using metaheuristic algorithms for solving the strains-from-conductivity inverse problem in a CNF-modified epoxy [275,282]. The CNF/epoxy was moulded in the shape of a plate with a hole and loaded in tension, causing strain concentrations in the vicinity of the hole. Genetic algorithms, simulated annealing and particle swarm optimization were explored because it was observed that the analytical formulation failed to converge to the physically correct solution for this more complex loading state. It was found that genetic algorithms performed the best for this inverse problem, but all methods compared favourably with DIC experimental validation. Because epoxy is relatively brittle, these studies were necessarily limited to infinitesimal strains. Despite the successes of the preceding studies, they were all limited to electro-mechanically isotropic materials. Translating these capabilities to electro-mechanically anisotropic materials remains a daunting challenge. Figure 7 summarizes results for strain recovery via piezoresistive inversion.

Some work has also been done for damage recovery via piezoresistive inversion. Recall that a key challenge with the damage recovery inverse problem is shape parameterization. To that end,

these preliminary studies have considered relatively simple damage cases. For example, various machine learning algorithms were used to categorize three damage conditions in a self-sensing bone cement directly from EIT boundary voltage data [283]. Thus, self-sensing materials also have overlap with machine learning methods (see §7). Bone cement is poly(methyl methacrylate) (PMMA) and is used to facilitate robust contact between an othopaedic implant (e.g. a total joint replacement) and hard bone. Failure of the PMMA interface is often difficult to detect via radiographic imaging, hence the motivation for alternative diagnostic tools. This clarification aside, the parameterization was relatively simple in this case—only four distinct states were possible (three damaged plus one healthy). The combination of EIT, self-sensing PMMA bone cement and machine learning allowed for correct damage classification with over 90% accuracy. In another study, image recognition-based machine learning was used to identify, size and localize through-hole damage to a self-sensing composite plate [284]. The image recognition algorithm was trained using computationally generated EIT images on a simple square domain punctured by a random number of randomly sized circular holes. The trained network was able to adeptly predict through-hole size, location and number from EIT conductivity maps with good accuracy—likely better accuracy than human interpretation of EIT images. But this again used a very simple damage parameterization (i.e. needing only to predict hole number, radius and in-plane coordinates). As a final example, a recent study looked at delamination shaping from EIT images in CNF-modified glass fibre/epoxy laminates [285]. In this study, delaminations induced by low-velocity impacts were parameterized as ellipses of unknown major and minor axes and centred at unknown in-plane coordinates. A genetic algorithm was used to inversely determine these parameters by minimizing the l_1-norm of the difference between experimentally collected EIT boundary voltage data and boundary voltage data predicted by a computational model of the damaged domain. Destructive analyses of the post-impacted laminates revealed that the genetic algorithm-predicted damage state much more closely matched the actual delamination size and shape than the EIT conductivity images. This third example of damage recovery is particularly noteworthy because it represents a much more realistic damage state.

In summary, this section has looked at smart, self-sensing materials from the perspective of structural inverse problems. Two noteworthy inverse problems were discussed—the EIT inverse problem and the strain/damage recovery problem. The former has been extensively researched in other fields (e.g. [286]). The latter, however, is much more recent and has only been the subject of a few precursory studies. Much work remains to be done regarding the inversion of electrical data to obtain underlying mechanical effects. Nonetheless, it can be seen that the field of smart materials in structural applications has much potential and cross-cutting overlap with other topics of this article, including extreme loading, SHM and machine learning.

7. A look forward: machine learning and education

This paper has evidenced the pervasiveness of inverse problems and methodologies used in the field of structural engineering. Yet, the following remains to question: What is guiding the future trajectory of inversion in structural engineering? In this section, we examine what we foresee as the two most influential future areas in addressing this question: machine learning and education.

(a) Machine-learned inversion

Many areas of structural engineering rely heavily on applied mathematics and science—from the integration of material models within finite-element frameworks to experimental measurement of structural response excitation. From a broad scientific perspective, there are two paradigms to research: either (i) the Keplerian paradigm (data driven, obtaining discoveries via data analysis) or (ii) the Newtonian paradigm (first principles, discovery through fundamental principles) [287]. Without question, structural engineering research uses both principles.

Often, first principles approaches are manifested via partial differential equations (PDEs) and their analytical or numerical solutions. However, in both research and practice, obtaining

solutions to PDEs can be infeasible or intractable, for example owing to computational demand, a dearth in available numerical regimes and/or the 'curse of dimensionality' [288]. In such cases where engineering problems are governed by such PDEs, solving a related inverse problem using a conventional methodology would also be a dubious task. When faced with this situation, we are most likely constrained to adopting a Keplerian approach.

Unmistakably, machine learning has provided the science and engineering communities with a powerful tool for data-driven analysis, prediction, assessment and significantly more. Structural engineering research has also greatly benefited from machine learning, especially in the areas of performance assessment [289], SHM [10] and analysis of various structural phenomena [290]. Yet, significantly less attention has been paid to the use of machine learning for solving inverse problems in structural engineering outside of areas such as SHM and NDE (as identified in §5).

Exemplifying this reality, structural design highly under-uses machine learning and data science. Design is traditionally associated with an iterative nature, in which various structural concepts are tested conceptually until a prevailing option is identified which adheres to constraints initially identified. The nature of this iterative design process has been understood in the past using positivist, pragmatic and post-modernist epistemologies ranging from Simon's 'science of the artificial' [291], Schön's 'reflexive practice' [292] and Buchanan's 'placements for contextualization' [293], respectively. The complexities involved in design from satisfying conflicting demands to exercising appropriate judgements is hence often attributed to being an innate human skill [56].

However, recent developments successfully solving inverse problems using data-driven approaches suggest that such methodologies could also be incorporated within structural design [25]. This challenges the notion that design is an exclusive human ability, a development which mimics the success of self-driving cars through data-driven approaches [294]. What is typically considered 'intuition' or 'engineering judgement' may in fact be recalling 'data points', committed to long-term memory through the process of experience, that are suitable solutions based on the unique set of constraints one is presented with [291]. Indeed, supervised machine learning was originally understood to create mapping functions that correlate a set of inputs (a specific set of constraints for a design situation) with associated outputs (viable structural solutions) by learning from a given dataset (experience) [295]. We note that this view has significantly evolved with the onset of deep learning, as well as the use of unsupervised and reinforcement learning regimes.

We therefore believe that this inverse problem perspective evidences the need for research on the development of machine learning tools for structural design. Data-driven approaches are often dismissed because they are 'black boxes' which lack a scientific rationale for their outputs. However, for design, this criticism might be unwarranted, and instead highlights the dogmatic concentration within academia on exclusively solving forward problems, which, owing to their well-posed nature, lend themselves to engineering science thinking. Recently, researchers have started investigating data-driven models. In one example, neural networks and clustering were applied to form a bridge and navigate the design space and shortlist viable and fitting solutions [296,297]. Other examples include researchers applying machine learning models to build suitable structural predictors for conceptual design related to building massing [298].

The former developments are, in our view, only a starting point for the employment of machine-learned models used in solving inverse problems in structural engineering as a new horizon of data-driven approaches emerge. Especially for the cases involving intractable forward problems, model reduction techniques have been promising [13,299–301], but these are either difficult to design by hand or are restricted by overly simplistic assumptions. Here, data-driven approaches are a powerful alternative to compensate for modelling errors [194,234,302] or reducing computational cost of iterative optimization schemes by model approximations [32,303]. Finally, we note that recent developments in geometric learning extend deep networks on Euclidean meshes to general meshes, such as finite elements, by a embedding them into graph structures essentially using the underlying geometry [304,305]. This opens the possibility to extend many data-driven approaches to complex structural problems.

(b) Inverse methodology in structural engineering education

Over the last 100 years, engineering education has experienced a number of fundamental shifts: a shift in focus away from design to engineering science in the 1960s, the rise of outcome-based accreditation in the UK and USA in the 1990s, along with a re-emphasis of teaching design through capstone projects in the 2000s [306]. There also is the continued tension between teaching graduates both the technical knowledge and the interpersonal skills demanded from industry deemed necessary to become effective designers [35]. To this day, there exists the debate on how to find the required balance between *knowledge-that* and *knowledge-how* as identified in §3 [307]. For civil and structural engineering disciplines, we believe that some of these challenges might be addressed by communicating the existence of inverse problems, their pervasive occurrences as shown by the sections above and teaching the various methods and techniques for solving such problems.

The dominance of engineering science within university curricula today, which primarily focuses on identifying and solving forward problems, might unintentionally generate the wrong supposition that all problems in engineering are well posed with idealized assumptions. Without adequately addressing the existence of inverse problems, and their distinctively qualitative differences from forward problems, it is easy to mistakenly assume that, for example, structural design is the application of such 'forward problems'. However, the idea that engineering is simply 'putting theory intro practice' [56] or 'applied science' [308] has been strongly argued against by numerous engineers and philosophers [55,309–311]. The challenge which students face when dealing with real-world design problems might be accounted for by the fact that, during the majority of their engineering education, they might lack a conceptual framework to adequately demarcate design from analysis. Similarly, in order to engage with other promising fields of structural engineering, such as SHM, blast engineering and smart materials, educating students on inverse problems is crucial.

Hence, a possible improvement for current civil and structural engineering curricula is introducing students to the existence of forward and inverse problems and how they relate to one another and to provide examples where each type of problem arises and how to solve them. As identified previously, this will also potentially require teaching students a host of new skills, especially if data-driven models continue to be effective tools for solving inverse problems, as is the case in SHM and increasingly likely in design. More importantly, especially when taking into consideration the recent developments in data science ranging from convolutional neural networks [312], transformers [313] and graph neural networks [314], there exists a vast spectrum of knowledge and applications we may not even be aware of.

As a matter of fact, in terms of research, we are perhaps faced with a unique situation in academia today. Although only time will tell, it could be argued that similar to how the 'invention' (or discovery) of calculus in the eighteenth century was instrumental in providing us with the necessary tools for solving forward problems, resulting in material models and PDEs which allow the creation of complex FEMs, so too might the rise of machine learning and data science, which are only now starting to gain serious attention in mathematics [287], allow a more rigorous treatment of solving inverse problems. By realizing the pervasiveness of inverse problems in structural engineering, but also the fundamental differences from forward problems, there is potentially a vast, untouched and exciting realm of research which awaits.

8. Conclusion

This article aimed to demonstrate that numerous structural engineering sub-fields may be either fundamentally or partially viewed as inverse problems. It was shown that this concept is well accepted in, for example, SHM; however, sub-fields such as structural design are not commonly (formally) defined as inverse problems. We argue that, by shifting this paradigm in structural engineering academia and industry, we may collectively capitalize on the rich methodologies and approaches already established in the inverse problems community. This beneficial relationship

between structural and inverse communities is expected to pay exponential dividends as new tools, such as machine-learned models, emerge and develop—offering new opportunities for solving previously inaccessible, intractable and/or unforeseen structural challenges.

Data accessibility. Data used in this article are available from the authors upon request.

Authors' contributions. A.G. and D.S. contributed equally to conceptualization of this work. All authors contributed to writing this article.

Competing interests. The authors declare that they have no competing interests.

Funding. A.H. is funded by Academy of Finland project nos. 338408 and 336796 (Finnish Centre of Excellence in Inverse Modelling and Imaging, 2018–2025). D.S. was supported by Engineering and Physical Sciences Research Council project no. EP/V007025/1. D.L. was supported by the National Natural Science Foundation of China under grant no. 61871356. A.G. was partially supported through the Ramboll Foundation PhD programme. X.K. was partially supported by the new faculty start-up research fund from the Gupta College of Science at Coastal Carolina University.

References

1. Reddy JN. 2019 *Introduction to the finite element method*. New York, NY: McGraw-Hill Education.
2. Surana KS, Reddy JN. 2016 *The finite element method for boundary value problems: mathematics and computations*. Boca Raton, FL: CRC Press.
3. Hughes TJ. 2012 *The finite element method: linear static and dynamic finite element analysis*. New York, NY: Dover Publications.
4. Zienkiewicz OC, Taylor RL, Nithiarasu P, Zhu J. 1977 *The finite element method*, vol. 3. London, UK: McGraw-Hill.
5. Virdi KS. 2006 Finite difference method for nonlinear analysis of structures. *J. Constr. Steel Res.* **62**, 1210–1218. (doi:10.1016/j.jcsr.2006.06.015)
6. Liszka T, Orkisz J. 1980 The finite difference method at arbitrary irregular grids and its application in applied mechanics. *Comput. Struct.* **11**, 83–95. (doi:10.1016/0045-7949(80)90149-2)
7. De Basabe JD, Sen MK. 2015 A comparison of finite-difference and spectral-element methods for elastic wave propagation in media with a fluid-solid interface. *Geophys. J. Int.* **200**, 278–298. (doi:10.1093/gji/ggu389)
8. Kudela P, Zak A, Krawczuk M, Ostachowicz W. 2007 Modelling of wave propagation in composite plates using the time domain spectral element method. *J. Sound Vib.* **302**, 728–745. (doi:10.1016/j.jsv.2006.12.016)
9. Griffith BE, Luo X. 2017 Hybrid finite difference/finite element immersed boundary method. *Int. J. Numer. Methods Biomed. Eng.* **33**, e2888.
10. Farrar CR, Worden K. 2012 *Structural health monitoring: a machine learning perspective*. Chichester, UK: John Wiley & Sons.
11. Liu GR, Han X. 2003 *Computational inverse techniques in nondestructive evaluation*. Boca Raton, FL: CRC Press.
12. Turco E. 2017 Tools for the numerical solution of inverse problems in structural mechanics: review and research perspectives. *Eur. J. Environ. Civil Eng.* **21**, 509–554. (doi:10.1080/19648189.2015.1134673)
13. Kaipio J, Somersalo E. 2006 *Statistical and computational inverse problems*, vol. 160. New York, NY: Springer Science & Business Media.
14. Adler J, Öktem O. 2017 Solving ill-posed inverse problems using iterative deep neural networks. *Inverse Prob.* **33**, 124007. (doi:10.1088/1361-6420/aa9581)
15. Calderon A. 1980 On an inverse boundary. In *Seminar on Numerical Analysis and its Applications to Continuum Physics, Rio de Janeiro, 1980*, pp. 65–73. Brazilian Math. Soc.
16. Tarantola A, Valette B. 1982 Inverse problems= quest for information. *J. Geophys.* **50**, 159–170.
17. Natterer F. 2001 *The mathematics of computerized tomography*. Philadelphia, PA: SIAM.
18. Mueller JL, Siltanen S. 2012 *Linear and nonlinear inverse problems with practical applications*. Philadelphia, PA: SIAM.
19. Engl HW, Hanke M, Neubauer A. 1996 *Regularization of inverse problems*, vol. 375. New York, NY: Springer Science & Business Media.
20. Nachman AI. 1988 Reconstructions from boundary measurements. *Ann. Math.* **128**, 531–576. (doi:10.2307/1971435)

21. Nachman AI. 1996 Global uniqueness for a two-dimensional inverse boundary value problem. *Ann. Math.* **143**, 71–96. (doi:10.2307/2118653)
22. Tikhonov AN, Arsenin VY. 1977 *Solutions of ill-posed problems*. New York, NY: John Wiley & Sons Inc.
23. Rudin LI, Osher S, Fatemi E. 1992 Nonlinear total variation based noise removal algorithms. *Physica D* **60**, 259–268. (doi:10.1016/0167-2789(92)90242-F)
24. Haber E, Ascher UM, Oldenburg D. 2000 On optimization techniques for solving nonlinear inverse problems. *Inverse Prob.* **16**, 1263. (doi:10.1088/0266-5611/16/5/309)
25. Arridge S, Maass P, Öktem O, Schönlieb CB. 2019 Solving inverse problems using data-driven models. *Acta Numerica* **28**, 1–174. (doi:10.1017/S0962492919000059)
26. Jin KH, McCann MT, Froustey E, Unser M. 2017 Deep convolutional neural network for inverse problems in imaging. *IEEE Trans. Image Process.* **26**, 4509–4522. (doi:10.1109/TIP.2017.2713099)
27. Kang I, Schulz MJ, Kim JH, Shanov V, Shi D. 2006 A carbon nanotube strain sensor for structural health monitoring. *Smart Mater. Struct.* **15**, 737. (doi:10.1088/0964-1726/15/3/009)
28. Hamilton SJ, Hauptmann A. 2018 Deep D-bar: real-time electrical impedance tomography imaging with deep neural networks. *IEEE Trans. Med. Imaging* **37**, 2367–2377. (doi:10.1109/TMI.2018.2828303)
29. Adler J, Öktem O. 2018 Learned primal-dual reconstruction. *IEEE Trans. Med. Imaging* **37**, 1322–1332. (doi:10.1109/TMI.2018.2799231)
30. Hammernik K, Klatzer T, Kobler E, Recht MP, Sodickson DK, Pock T, Knoll F. 2018 Learning a variational network for reconstruction of accelerated MRI data. *Magn. Reson. Med.* **79**, 3055–3071. (doi:10.1002/mrm.26977)
31. Hauptmann A, Lucka F, Betcke M, Huynh N, Adler J, Cox B, Beard P, Ourselin S, Arridge S. 2018 Model-based learning for accelerated, limited-view 3-D photoacoustic tomography. *IEEE Trans. Med. Imaging* **37**, 1382–1393. (doi:10.1109/TMI.2018.2820382)
32. Smyl D, Tallman TN, Liu D, Hauptmann A. 2021 An efficient quasi-Newton method for nonlinear inverse problems via learned singular values. *IEEE Signal Process Lett.* **28**, 748–752. (doi:10.1109/LSP.2021.3063622)
33. Zhang J, Ghanem B. 2018 ISTA-Net: Interpretable optimization-inspired deep network for image compressive sensing. In *Proc. IEEE Conf. on Computer Vision and Pattern Recognition*, pp. 1828–1837.
34. Monga V, Li Y, Eldar YC. 2021 Algorithm unrolling: interpretable, efficient deep learning for signal and image processing. *IEEE Signal Process Mag.* **38**, 18–44. (doi:10.1109/MSP.2020.3016905)
35. Crawley E, Malmqvist J, Ostlund S, Brodeur D, Edstrom K. 2007 Rethinking engineering education. *The CDIO Approach* **302**, 60–62.
36. Seely BE. 1999 The other re-engineering of engineering education, 1900–1965. *J. Eng. Educ.* **88**, 285–294. (doi:10.1002/j.2168-9830.1999.tb00449.x)
37. Mann A. 2016 *Historical development of structural theories and methods of modern computer*. London, UK: Institution of Structural Engineers.
38. Coleman E, Shealy T, Grohs J, Godwin A. 2020 Design thinking among first-year and senior engineering students: a cross-sectional, national study measuring perceived ability. *J. Eng. Educ.* **109**, 72–87. (doi:10.1002/jee.20298)
39. Bulleit W, Schmidt J, Alvi I, Nelson E, Rodriguez-Nikl T. 2015 Philosophy of engineering: what it is and why it matters. *J. Prof. Issues Eng. Educ. Practice* **141**, 1–9.
40. Simon HA. 1973 The structure of ill structured problems. *Artif. Intell.* **4**, 181–201. (doi:10.1016/0004-3702(73)90011-8)
41. Dym CL, Agogino AM, Eris O, Frey DD, Leifer LJ. 2006 Engineering design thinking, teaching, and learning. *IEEE Eng. Manage. Rev.* **34**, 65–90. (doi:10.1109/EMR.2006.1679078)
42. Rittel HWJ, Webber MM. 1973 Dilemmas in a general theory of planning. *Policy Sci.* **4**, 155–169. (doi:10.1007/BF01405730)
43. Mason JC, Manning MW, Cormie AM, Johnston JS, Low AM, Merlbourne C, Nicholl RD, Ryland MF, Weare FE. 2018 *Structural design—the engineer's role*, 2nd edn. London, UK: Institution of Structural Engineers.
44. Alifanov OM. 1983 Methods of solving ill-posed inverse problems. *J. Eng. Phys.* **45**, 1237–1245. (doi:10.1007/BF01254725)
45. Yang JN. 1975 Application of optimal control theory to civil engineering structures. *J. Eng. Mech. Div.* **101**, 819–838. (doi:10.1061/JMCEA3.0002075)

46. Wise C. 2016 *Introduction: part 1. Structure is everywhere!*. London, UK: The Institution of Structural Engineers.
47. Rombouts J, Liew A, Lombaert G, De Laet L, Block P, Schevenels M. 2021 Designing bending-active gridshells as falsework for concrete shells through numerical optimization. *Eng. Struct.* **240**, 112352. (doi:10.1016/j.engstruct.2021.112352)
48. Liew A, Stürz YR, Guillaume S, Van Mele T, Smith RS, Block P. 2018 Active control of a rod-net formwork system prototype. *Autom. Constr.* **96**, 128–140. (doi:10.1016/j.autcon.2018.09.002)
49. Van Mele T, Panozzo D, Sorkine-Hornung O, Block P. 2014 Best-fit thrust network analysis–rationalization of freeform meshes. In *Shell structures for architecture: form finding and optimization* (eds S Adriaenssens, P Block, D Veenendaal, C Williams). London, UK: Routledge.
50. Fairclough HE, Gilbert M, Pichugin AV, Tyas A, Firth I. 2018 Theoretically optimal forms for very long-span bridges under gravity loading. *Proc. R. Soc. A* **474**, 20170726. (doi:10.1098/rspa.2017.0726)
51. Liew A. 2020 Constrained force density method optimisation for compression-only shell structures. *Structures* **28**, 1845–1856. (doi:10.1016/j.istruc.2020.09.078)
52. He L, Gilbert M. 2015 Rationalization of trusses generated via layout optimization. *Struct. Multidiscip. Optim.* **52**, 677–694. (doi:10.1007/s00158-015-1260-x)
53. McKinstray R, Lim JB, Tanyimboh TT, Phan DT, Sha W. 2015 Optimal design of long-span steel portal frames using fabricated beams. *J. Constr. Steel Res.* **104**, 104–114. (doi:10.1016/j.jcsr.2014.10.010)
54. Ye J, Becque J, Hajirasouliha I, Mojtabaei SM, Lim JBP. 2018 Development of optimum cold-formed steel sections for maximum energy dissipation in uniaxial bending. *Eng. Struct.* **161**, 55–67. (doi:10.1016/j.engstruct.2018.01.070)
55. Koen BV. 2003 *Discussion of the method: conducting the engineer's approach to problem solving*. New York, NY: Oxford University Press.
56. Addis W. 1990 *Structural engineering: the nature of theory and design*. Chichester, UK: Ellis Horwood Limited.
57. Cormie D, Mays G, Smith P. 2009 *Blast effects on buildings*, 2nd edn. London, UK: Thomas Telford.
58. Rigby SE, Lodge TJ, Alotaibi S, Barr AD, Clarke SD, Langdon GS, Tyas A. 2020 Preliminary yield estimation of the 2020 Beirut explosion using video footage from social media. *Shock Waves* **30**, 671–675. (doi:10.1007/s00193-020-00970-z)
59. Ambrosini D, Luccioni B, Jacinto A, Danesi R. 2005 Location and mass of explosive from structural damage. *Eng. Struct.* **27**, 167–176. (doi:10.1016/j.engstruct.2004.09.003)
60. van der Voort MM, van Wees RMM, Brouwer SD, van der Jagt-Deutekom MJ, Verreault J. 2015 Forensic analysis of explosions: inverse calculation of the charge mass. *Forensic Sci. Int.* **252**, 11–21. (doi:10.1016/j.forsciint.2015.04.014)
61. Clarke SD, Fay SD, Warren JA, Tyas A, Rigby SE, Elgy I. 2015 A large scale experimental approach to the measurement of spatially and temporally localised loading from the detonation of shallow-buried explosives. *Meas. Sci. Technol.* **26**, 015001. (doi:10.1088/0957-0233/26/1/015001)
62. Rigby SE, Tyas A, Clarke SD, Fay SD, Reay JJ, Warren JA, Gant M, Elgy I. 2015 Observations from preliminary experiments on spatial and temporal pressure measurements from near-field free air explosions. *Int. J. Protective Struct.* **6**, 175–190. (doi:10.1260/2041-4196.6.2.175)
63. Curry RJ, Langdon GS. 2017 Transient response of steel plates subjected to close proximity explosive detonations in air. *Int. J. Impact Eng.* **102**, 102–116. (doi:10.1016/j.ijimpeng.2016.12.004)
64. Rigby SE, Tyas A, Curry RJ, Langdon GS. 2019 Experimental measurement of specific impulse distribution and transient deformation of plates subjected to near-field explosive blasts. *Exp. Mech.* **59**, 163–178. (doi:10.1007/s11340-018-00438-3)
65. Rigby SE, Akintaro OI, Fuller BJ, Tyas A, Curry RJ, Langdon GS, Pope DJ. 2019 Predicting the response of plates subjected to near-field explosions using an energy equivalent impulse. *Int. J. Impact Eng.* **128**, 24–36. (doi:10.1016/j.ijimpeng.2019.01.014)
66. Pannell JJ, Panoutsos G, Cooke SB, Pope DJ, Rigby SE. 2021 Predicting specific impulse distributions for spherical explosives in the extreme near-field using a Gaussian function. *Int. J. Prot. Struct.* **12**, 437–459. (doi:10.1177/2041419621993492)

67. Xu S, Deng X, Tiwari V, Sutton MA, Fourney WL, Bretall D. 2010 An inverse approach for pressure load identification. *Int. J. Impact Eng.* **37**, 865–877. (doi:10.1016/j.ijimpeng.2009.10.007)
68. Xu S, Tiwari V, Deng X, Sutton MA, Fourney WL. 2011 Identification of interaction pressure between structure and explosive with inverse approach. *Exp. Mech.* **51**, 815–830. (doi:10.1007/s11340-010-9390-y)
69. Langran-Wheeler C, Rigby S, Clarke SD, Tyas A, Stephens C, Walker R. 2021 Near-field spatial and temporal blast pressure distributions from non-spherical charges: horizontally-aligned cylinders. *Int. J. Prot. Struct.* **12**, 492–516. (doi:10.1177/20414196211013443)
70. Tyas A, Reay JJ, Fay SD, Clarke SD, Rigby SE, Warren JA, Pope DJ. 2016 Experimental studies of the effect of rapid afterburn on shock development of near-field explosions. *Int. J. Prot. Struct.* **7**, 456–465. (doi:10.1177/2041419616665931)
71. Rigby SE, Knighton R, Clarke SD, Tyas A. 2020 Reflected near-field blast pressure measurements using high speed video. *Exp. Mech.* **60**, 875–888. (doi:10.1007/s11340-020-00615-3)
72. Rigby SE, Fay SD, Tyas A, Clarke SD, Reay JJ, Warren JA, Gant M, Elgy I. 2018 Influence of particle size distribution on the blast pressure profile from explosives buried in saturated soils. *Shock Waves* **28**, 613–626. (doi:10.1007/s00193-017-0727-7)
73. Friswell MI. 2007 Damage identification using inverse methods. *Phil. Trans. R. Soc. A* **365**, 393–410. (doi:10.1098/rsta.2006.1930)
74. Kerschen G, Worden K, Vakakis AF, Golinval JC. 2006 Past, present and future of nonlinear system identification in structural dynamics. *Mech. Syst. Signal Process.* **20**, 505–592. (doi:10.1016/j.ymssp.2005.04.008)
75. Sinha JK, Friswell M, Edwards S. 2002 Simplified models for the location of cracks in beam structures using measured vibration data. *J. Sound Vib.* **251**, 13–38. (doi:10.1006/jsvi.2001.3978)
76. Sinou JJ. 2009 A review of damage detection and health monitoring of mechanical systems from changes in the measurement of linear and non-linear vibrations. In *Mechanical vibrations: measurement, effects and control* (ed. RC Sapri), pp. 643–702. Hauppauge, NY: Nova Science Publishers, Inc.
77. Farhat C, Hemez FM. 1993 Updating finite element dynamic models using an element-by-element sensitivity methodology. *AIAA J.* **31**, 1702–1711. (doi:10.2514/3.11833)
78. Ricles J, Kosmatka J. 1992 Damage detection in elastic structures using vibratory residual forces and weighted sensitivity. *AIAA J.* **30**, 2310–2316. (doi:10.2514/3.11219)
79. Lin HP. 2004 Direct and inverse methods on free vibration analysis of simply supported beams with a crack. *Eng. Struct.* **26**, 427–436. (doi:10.1016/j.engstruct.2003.10.014)
80. Hester D, González A. 2012 A wavelet-based damage detection algorithm based on bridge acceleration response to a vehicle. *Mech. Syst. Signal Process.* **28**, 145–166. (doi:10.1016/j.ymssp.2011.06.007)
81. Hadjileontiadis L, Douka E, Trochidis A. 2005 Fractal dimension analysis for crack identification in beam structures. *Mech. Syst. Signal Process.* **19**, 659–674. (doi:10.1016/j.ymssp.2004.03.005)
82. Pawar PM, Ganguli R. 2003 Genetic fuzzy system for damage detection in beams and helicopter rotor blades. *Comput. Methods Appl. Mech. Eng.* **192**, 2031–2057. (doi:10.1016/S0045-7825(03)00237-8)
83. Lourens E, Reynders E, De Roeck G, Degrande G, Lombaert G. 2012 An augmented Kalman filter for force identification in structural dynamics. *Mech. Syst. Signal Process.* **27**, 446–460. (doi:10.1016/j.ymssp.2011.09.025)
84. Nichols J, Trickey S, Todd M, Virgin L. 2003 Structural health monitoring through chaotic interrogation. *Meccanica* **38**, 239–250. (doi:10.1023/A:1022898403359)
85. Liu J, Sun X, Han X, Jiang C, Yu D. 2014 A novel computational inverse technique for load identification using the shape function method of moving least square fitting. *Comput. Struct.* **144**, 127–137. (doi:10.1016/j.compstruc.2014.08.002)
86. Nasrellah H, Manohar C. 2010 A particle filtering approach for structural system identification in vehicle–structure interaction problems. *J. Sound Vib.* **329**, 1289–1309. (doi:10.1016/j.jsv.2009.10.041)
87. Ebrahimian H, Astroza R, Conte JP, Papadimitriou C. 2018 Bayesian optimal estimation for output-only nonlinear system and damage identification of civil structures. *Struct. Control Health Monit.* **25**, e2128. (doi:10.1002/stc.2128)

88. Farrar CR, Worden K. 2007 An introduction to structural health monitoring. *Phil. Trans. R. Soc. A* **365**, 303–315. (doi:10.1098/rsta.2006.1928)
89. Worden K, Farrar CR, Haywood J, Todd M. 2008 A review of nonlinear dynamics applications to structural health monitoring. *Struct. Control Health Monit.: The Official J. Int. Assoc. Struct. Control and Monit. and of the European Assoc. Control of Struct.* **15**, 540–567.
90. Huang L, Zeng L, Lin J. 2017 Baseline-free damage detection in composite plates based on the reciprocity principle. *Smart Mater. Struct.* **27**, 015026. (doi:10.1088/1361-665X/aa9cc1)
91. Sohn H, Park HW, Law KH, Farrar CR. 2007 Combination of a time reversal process and a consecutive outlier analysis for baseline-free damage diagnosis. *J. Intell. Mater. Syst. Struct.* **18**, 335–346. (doi:10.1177/1045389X0606629)
92. Santos JP, Orcesi AD, Crémona C, Silveira P. 2015 Baseline-free real-time assessment of structural changes. *Struct. Infrastructure Eng.* **11**, 145–161. (doi:10.1080/15732479.2013.858169)
93. Anton SR, Inman DJ, Park G. 2009 Reference-free damage detection using instantaneous baseline measurements. *AIAA J.* **47**, 1952–1964. (doi:10.2514/1.43252)
94. Inaudi D. 2010 Long-term static structural health monitoring. In *Structures Congress 2010*, pp. 566–577.
95. Downey A, D'Alessandro A, Baquera M, García-Macías E, Rolfes D, Ubertini F, Laflamme S, Castro-Triguero R. 2017 Damage detection, localization and quantification in conductive smart concrete structures using a resistor mesh model. *Eng. Struct.* **148**, 924–935. (doi:10.1016/j.engstruct.2017.07.022)
96. Zhou Z, Liu W, Huang Y, Wang H, Jianping H, Huang M, Jinping O. 2012 Optical fiber Bragg grating sensor assembly for 3D strain monitoring and its case study in highway pavement. *Mech. Syst. Signal Process.* **28**, 36–49. (doi:10.1016/j.ymssp.2011.10.003)
97. Lecompte D, Smits AS, Bossuyt S, Sol H, Vantomme J, Van Hemelrijck D, Habraken AM. 2006 Quality assessment of speckle patterns for digital image correlation. *Opt. Lasers Eng.* **44**, 1132–1145. (doi:10.1016/j.optlaseng.2005.10.004)
98. Borcea L. 2002 Electrical impedance tomography. *Inverse Prob.* **18**, R99. (doi:10.1088/0266-5611/18/6/201)
99. Zare Hosseinzadeh A, Ghodrati Amiri G, Koo KY. 2016 Optimization-based method for structural damage localization and quantification by means of static displacements computed by flexibility matrix. *Eng. Optim.* **48**, 543–561. (doi:10.1080/0305215X.2015.1017476)
100. Kefal A, Oterkus E. 2016 Displacement and stress monitoring of a Panamax containership using inverse finite element method. *Ocean Eng.* **119**, 16–29. (doi:10.1016/j.oceaneng.2016.04.025)
101. Sanayei M, Khaloo A, Gul M, Catbas FN. 2015 Automated finite element model updating of a scale bridge model using measured static and modal test data. *Eng. Struct.* **102**, 66–79. (doi:10.1016/j.engstruct.2015.07.029)
102. Ni B, Gao H. 2021 A deep learning approach to the inverse problem of modulus identification in elasticity. *MRS Bull.* **46**, 19–25. (doi:10.1557/s43577-020-00006-y)
103. Waeytens J, Rosic B, Charbonnel PE, Merliot E, Siegert D, Chapeleau X, Vidal R, Le Corvec V, Cottineau LM. 2016 Model updating techniques for damage detection in concrete beam using optical fiber strain measurement device. *Eng. Struct.* **129**, 2–10. (doi:10.1016/j.engstruct.2016.08.004)
104. Ruybalid AP, Hoefnagels JP, van der Sluis O, Geers MG. 2016 Comparison of the identification performance of conventional FEM updating and integrated DIC. *Int. J. Numer. Methods Eng.* **106**, 298–320. (doi:10.1002/nme.5127)
105. Karageorghis A, Lesnic D, Marin L. 2016 The method of fundamental solutions for three-dimensional inverse geometric elasticity problems. *Comput. Struct.* **166**, 51–59. (doi:10.1016/j.compstruc.2016.01.010)
106. Mathieu F, Leclerc H, Hild F, Roux S. 2015 Estimation of elastoplastic parameters via weighted FEMU and integrated-DIC. *Exp. Mech.* **55**, 105–119. (doi:10.1007/s11340-014-9888-9)
107. Kefal A, Oterkus E, Tessler A, Spangler JL. 2016 A quadrilateral inverse-shell element with drilling degrees of freedom for shape sensing and structural health monitoring. *Eng. Sci. Technol., Int. J.* **19**, 1299–1313. (doi:10.1016/j.jestch.2016.03.006)

108. Smyl D, Antin KN, Liu D, Bossuyt S. 2018 Coupled digital image correlation and quasi-static elasticity imaging of inhomogeneous orthotropic composite structures. *Inverse Prob.* **34**, 124005. (doi:10.1088/1361-6420/aae793)
109. Shen B, Stanciulescu I, Paulino GH. 2010 Inverse computation of cohesive fracture properties from displacement fields. *Inverse Problems Sci. Eng.* **18**, 1103–1128. (doi:10.1080/17415977.2010.512661)
110. Xu ZH, Yang Y, Huang P, Li X. 2010 Determination of interfacial properties of thermal barrier coatings by shear test and inverse finite element method. *Acta Mater.* **58**, 5972–5979. (doi:10.1016/j.actamat.2010.07.013)
111. Avril S *et al.* 2008 Overview of identification methods of mechanical parameters based on full-field measurements. *Exp. Mech.* **48**, 381–402. (doi:10.1007/s11340-008-9148-y)
112. Lecampion B, Gunning J. 2007 Model selection in fracture mapping from elastostatic data. *Int. J. Solids Struct.* **44**, 1391–1408. (doi:10.1016/j.ijsolstr.2006.06.022)
113. Amiot F, Hild F, Roger JP. 2007 Identification of elastic property and loading fields from full-field displacement measurements. *Int. J. Solids Struct.* **44**, 2863–2887. (doi:10.1016/j.ijsolstr.2006.08.031)
114. Hild F, Roux S. 2006 Digital image correlation: from displacement measurement to identification of elastic properties–a review. *Strain* **42**, 69–80. (doi:10.1111/j.1475-1305.2006.00258.x)
115. Bonnet M, Constantinescu A. 2005 Inverse problems in elasticity. *Inverse Prob.* **21**, R1. (doi:10.1088/0266-5611/21/2/R01)
116. Morassi A, Rosset E. 2004 Stable determination of cavities in elastic bodies. *Inverse Prob.* **20**, 453. (doi:10.1088/0266-5611/20/2/010)
117. Maniatty A, Zabaras N, Stelson K. 1989 Finite element analysis of some inverse elasticity problems. *J. Eng. Mech.* **115**, 1303–1317. (doi:10.1061/(ASCE)0733-9399(1989)115:6(1303))
118. Gomes GF, Pereira JVP. 2020 Sensor placement optimization and damage identification in a fuselage structure using inverse modal problem and firefly algorithm. *Evol. Intell.* **13**, 571–591. (doi:10.1007/s12065-020-00372-1)
119. An Y, Chatzi E, Sim SH, Laflamme S, Blachowski B, Ou J. 2019 Recent progress and future trends on damage identification methods for bridge structures. *Struct. Control Health Monit.* **26**, e2416.
120. Colombo L, Sbarufatti C, Giglio M. 2019 Definition of a load adaptive baseline by inverse finite element method for structural damage identification. *Mech. Syst. Signal Process.* **120**, 584–607. (doi:10.1016/j.ymssp.2018.10.041)
121. Amanzadeh M, Aminossadati SM, Kizil MS, Rakić AD. 2018 Recent developments in fibre optic shape sensing. *Measurement* **128**, 119–137. (doi:10.1016/j.measurement.2018.06.034)
122. Di Sante R. 2015 Fibre optic sensors for structural health monitoring of aircraft composite structures: recent advances and applications. *Sensors* **15**, 18 666–18 713. (doi:10.3390/s150818666)
123. Cerracchio P, Gherlone M, Di Sciuva M, Tessler A. 2015 A novel approach for displacement and stress monitoring of sandwich structures based on the inverse finite element method. *Compos. Struct.* **127**, 69–76. (doi:10.1016/j.compstruct.2015.02.081)
124. Gherlone M, Cerracchio P, Mattone M, Di Sciuva M, Tessler A. 2014 An inverse finite element method for beam shape sensing: theoretical framework and experimental validation. *Smart Mater. Struct.* **23**, 045027. (doi:10.1088/0964-1726/23/4/045027)
125. Derkevorkian A, Masri SF, Alvarenga J, Boussalis H, Bakalyar J, Richards WL. 2013 Strain-based deformation shape-estimation algorithm for control and monitoring applications. *AIAA J.* **51**, 2231–2240. (doi:10.2514/1.J052215)
126. Weisz-Patrault D, Ehrlacher A, Legrand N. 2013 Evaluation of contact stress during rolling process, by three dimensional analytical inverse method. *Int. J. Solids Struct.* **50**, 3319–3331. (doi:10.1016/j.ijsolstr.2013.06.005)
127. Gherlone M, Cerracchio P, Mattone M, Di Sciuva M, Tessler A. 2012 Shape sensing of 3D frame structures using an inverse finite element method. *Int. J. Solids Struct.* **49**, 3100–3112. (doi:10.1016/j.ijsolstr.2012.06.009)
128. Tessler A, Spangler JL, Gherlone M, Mattone M, Di Sciuva M. 2011 *Real-time characterization of aerospace structures using onboard strain measurement technologies and inverse finite element method*. Hampton, VA: National Aeronautics and Space Administration VA Langley Research Center.

129. Kiesel S, Van Vickle P, Peters KJ, Hassan T, Kowalsky M. 2006 Intrinsic polymer optical fiber sensors for high-strain applications. In *Smart Structures and Materials 2006: Smart Sensor Monitoring Systems and Applications*, vol. 6167, p. 616713. International Society for Optics and Photonics.
130. Song JH, Lee ET, Eun HC. 2021 Optimal sensor placement through expansion of static strain measurements to static displacements. *Int. J. Distrib. Sens. Netw.* **17**, 1550147721991712. (doi:10.1177/1550147721991712)
131. Esposito M, Gherlone M. 2020 Composite wing box deformed-shape reconstruction based on measured strains: optimization and comparison of existing approaches. *Aerosp. Sci. Technol.* **99**, 105758. (doi:10.1016/j.ast.2020.105758)
132. Ostachowicz W, Soman R, Malinowski P. 2019 Optimization of sensor placement for structural health monitoring: a review. *Struct. Health Monit.* **18**, 963–988. (doi:10.1177/1475921719825601)
133. Tenreiro AFG, Lopes AM. 2021 A review of structural health monitoring of bonded structures using electromechanical impedance spectroscopy. *Struct. Health Monit.* (doi:10.1177/1475921721993419)
134. Alessandrini G, Morassi A, Rosset E. 2002 Detecting cavities by electrostatic boundary measurements. *Inverse Prob.* **18**, 1333. (doi:10.1088/0266-5611/18/5/308)
135. Downey A, D'Alessandro A, Laflamme S, Ubertini F. 2017 Smart bricks for strain sensing and crack detection in masonry structures. *Smart Mater. Struct.* **27**, 015009. (doi:10.1088/1361-665X/aa98c2)
136. Sadoughi M, Downey A, Yan J, Hu C, Laflamme S. 2018 Reconstruction of unidirectional strain maps via iterative signal fusion for mesoscale structures monitored by a sensing skin. *Mech. Syst. Signal Process.* **112**, 401–416. (doi:10.1016/j.ymssp.2018.04.023)
137. Kong X, Li J, Collins W, Bennett C, Laflamme S, Jo H. 2018 Sensing distortion-induced fatigue cracks in steel bridges with capacitive skin sensor arrays. *Smart Mater. Struct.* **27**, 115008. (doi:10.1088/1361-665X/aadbfb)
138. Kong X, Li J, Collins W, Bennett C, Laflamme S, Jo H. 2017 A large-area strain sensing technology for monitoring fatigue cracks in steel bridges. *Smart Mater. Struct.* **26**, 085024. (doi:10.1088/1361-665X/aa75ef)
139. Downey A, Laflamme S, Ubertini F. 2016 Reconstruction of in-plane strain maps using hybrid dense sensor network composed of sensing skin. *Meas. Sci. Technol.* **27**, 124016. (doi:10.1088/0957-0233/27/12/124016)
140. Voss A, Hosseini P, Pour-Ghaz M, Vauhkonen M, Seppänen A. 2019 Three-dimensional electrical capacitance tomography – a tool for characterizing moisture transport properties of cement-based materials. *Mater. Des.* **181**, 107967. (doi:10.1016/j.matdes.2019.107967)
141. Grudzien K, Chaniecki Z, Romanowski A, Sankowski D, Nowakowski J, Niedostatkiewicz M. 2016 Application of twin-plane ECT sensor for identification of the internal imperfections inside concrete beams. In *2016 IEEE Int. Instrumentation and Measurement Technology Conf. Proc.*, pp. 1–6.
142. Smyl D, Pour-Ghaz M, Seppänen A. 2018 Detection and reconstruction of complex structural cracking patterns with electrical imaging. *NDT & E Int.* **99**, 123–133. (doi:10.1016/j.ndteint.2018.06.004)
143. Seppänen A, Hallaji M, Pour-Ghaz M. 2017 A functionally layered sensing skin for the detection of corrosive elements and cracking. *Struct. Health Monit.* **16**, 215–224. (doi:10.1177/1475921716670574)
144. Karhunen K, Seppänen A, Lehikoinen A, Monteiro PJM, Kaipio JP. 2010 Electrical resistance tomography imaging of concrete. *Cement Concrete Res.* **40**, 137–145. (doi:10.1016/j.cemconres.2009.08.023)
145. Rashetnia R, Hallaji M, Smyl D, Seppänen A, Pour-Ghaz M. 2017 Detection and localization of changes in two-dimensional temperature distributions by electrical resistance tomography. *Smart Mater. Struct.* **26**, 115021. (doi:10.1088/1361-665X/aa8f75)
146. Hauptmann A, Smyl D. 2021 Fusing electrical and elasticity imaging. *Phil. Trans. R. Soc. A* **379**, 20200194. (doi:10.1098/rsta.2020.0194)
147. Bao Y, Chen Z, Wei S, Xu Y, Tang Z, Li H. 2019 The state of the art of data science and engineering in structural health monitoring. *Engineering* **5**, 234–242. (doi:10.1016/j.eng.2018.11.027)

148. Fan X, Li J, Hao H, Ma S. 2018 Identification of minor structural damage based on electromechanical impedance sensitivity and sparse regularization. *J. Aerosp. Eng.* **31**, 04018061. (doi:10.1061/(ASCE)AS.1943-5525.0000892)
149. Kim J, Wang KW. 2019 Electromechanical impedance-based damage identification enhancement using bistable and adaptive piezoelectric circuitry. *Struct. Health Monit.* **18**, 1268–1281. (doi:10.1177/1475921718794202)
150. Brownjohn JM. 2007 Structural health monitoring of civil infrastructure. *Phil. Trans. R. Soc. A* **365**, 589–622. (doi:10.1098/rsta.2006.1925)
151. Entezami A, Shariatmadar H. 2019 Structural health monitoring by a new hybrid feature extraction and dynamic time warping methods under ambient vibration and non-stationary signals. *Measurement* **134**, 548–568. (doi:10.1016/j.measurement.2018.10.095)
152. Ramos LF, Aguilar R, Lourenço PB, Moreira S. 2013 Dynamic structural health monitoring of Saint Torcato church. *Mech. Syst. Signal Process.* **35**, 1–15. (doi:10.1016/j.ymssp.2012.09.007)
153. Magalhães F. 2012 Vibration based structural health monitoring of an arch bridge: from automated OMA to damage detection. *Mech. Syst. Signal Process.* **28**, 212–228. (doi:10.1016/j.ymssp.2011.06.011)
154. Nagarajaiah S, Yang Y. 2017 Modeling and harnessing sparse and low-rank data structure: a new paradigm for structural dynamics, identification, damage detection, and health monitoring. *Struct. Control Health Monit.* **24**, e1851. (doi:10.1002/stc.1851)
155. Koo KY, Brownjohn J, List D, Cole R. 2013 Structural health monitoring of the Tamar suspension bridge. *Struct. Control Health Monit.* **20**, 609–625. (doi:10.1002/stc.1481)
156. Marcuzzi A, Morassi A. 2010 Dynamic identification of a concrete bridge with orthotropic plate-type deck. *J. Struct. Eng.* **136**, 586–602. (doi:10.1061/(ASCE)ST.1943-541X.0000146)
157. Pines D, Salvino L. 2006 Structural health monitoring using empirical mode decomposition and the Hilbert phase. *J. Sound Vib.* **294**, 97–124. (doi:10.1016/j.jsv.2005.10.024)
158. Hong YH, Kim HK, Lee HS. 2010 Reconstruction of dynamic displacement and velocity from measured accelerations using the variational statement of an inverse problem. *J. Sound Vib.* **329**, 4980–5003. (doi:10.1016/j.jsv.2010.05.016)
159. Wan Z, Li S, Huang Q, Wang T. 2014 Structural response reconstruction based on the modal superposition method in the presence of closely spaced modes. *Mech. Syst. Signal Process.* **42**, 14–30. (doi:10.1016/j.ymssp.2013.07.007)
160. Paul B, George RC, Mishra SK. 2017 Phase space interrogation of the empirical response modes for seismically excited structures. *Mech. Syst. Signal Process.* **91**, 250–265. (doi:10.1016/j.ymssp.2016.12.008)
161. Nichols J, Todd M, Wait J. 2003 Using state space predictive modeling with chaotic interrogation in detecting joint preload loss in a frame structure experiment. *Smart Mater. Struct.* **12**, 580. (doi:10.1088/0964-1726/12/4/310)
162. Fernández-Sáez J, Morassi A, Rubio L. 2017 The λ-curves method for crack identification in beams. *Procedia Eng.* **199**, 1964–1969. (doi:10.1016/j.proeng.2017.09.304)
163. Liu G, Mao Z, Todd M, Huang Z. 2014 Damage assessment with state–space embedding strategy and singular value decomposition under stochastic excitation. *Struct. Health Monit.* **13**, 131–142. (doi:10.1177/1475921713513973)
164. Yao R, Pakzad SN. 2012 Autoregressive statistical pattern recognition algorithms for damage detection in civil structures. *Mech. Syst. Signal Process.* **31**, 355–368. (doi:10.1016/j.ymssp.2012.02.014)
165. Nair KK, Kiremidjian AS, Law KH. 2006 Time series-based damage detection and localization algorithm with application to the ASCE benchmark structure. *J. Sound Vib.* **291**, 349–368. (doi:10.1016/j.jsv.2005.06.016)
166. Dervilis N, Shi H, Worden K, Cross E. 2016 Exploring environmental and operational variations in SHM data using heteroscedastic Gaussian processes. In *Dynamics of civil structures*, vol. 2, pp. 145–153. New York, NY: Springer.
167. Ramancha MK, Astroza R, Conte JP, Restrepo JI, Todd MD. 2020 Bayesian nonlinear finite element model updating of a full-scale bridge-column using sequential Monte Carlo. In *Model validation and uncertainty quantification*, vol. 3, pp. 389–397. New York, NY: Springer.
168. Wan HP, Ni YQ. 2019 Bayesian multi-task learning methodology for reconstruction of structural health monitoring data. *Struct. Health Monit.* **18**, 1282–1309. (doi:10.1177/1475921718794953)
169. Wan HP, Ren WX. 2016 Stochastic model updating utilizing Bayesian approach and Gaussian process model. *Mech. Syst. Signal Process.* **70**, 245–268. (doi:10.1016/j.ymssp.2015.08.011)

170. Mao Z, Todd M. 2013 Statistical modeling of frequency response function estimation for uncertainty quantification. *Mech. Syst. Signal Process.* **38**, 333–345. (doi:10.1016/j.ymssp.2013.01.021)
171. Cantero-Chinchilla S, Beck JL, Chiachío M, Chiachío J, Chronopoulos D, Jones A. 2020 Optimal sensor and actuator placement for structural health monitoring via an efficient convex cost-benefit optimization. *Mech. Syst. Signal Process.* **144**, 106901. (doi:10.1016/j.ymssp.2020.106901)
172. Capellari G, Chatzi E, Mariani S. 2018 Cost–benefit optimization of structural health monitoring sensor networks. *Sensors* **18**, 2174. (doi:10.3390/s18072174)
173. Yi TH, Li HN, Wang CW. 2016 Multiaxial sensor placement optimization in structural health monitoring using distributed Wolf algorithm. *Struct. Control Health Monit.* **23**, 719–734. (doi:10.1002/stc.1806)
174. Sun H, Büyüköztürk O. 2015 Optimal sensor placement in structural health monitoring using discrete optimization. *Smart Mater. Struct.* **24**, 125034. (doi:10.1088/0964-1726/24/12/125034)
175. Bhuiyan MZA, Wang G, Cao J, Wu J. 2014 Sensor placement with multiple objectives for structural health monitoring. *ACM Trans. Sensor Netw. (TOSN)* **10**, 1–45. (doi:10.1145/2533669)
176. Yi TH, Li HN, Zhang XD. 2012 A modified monkey algorithm for optimal sensor placement in structural health monitoring. *Smart Mater. Struct.* **21**, 105033. (doi:10.1088/0964-1726/21/10/105033)
177. Yi TH, Li HN, Gu M. 2011 Optimal sensor placement for structural health monitoring based on multiple optimization strategies. *Struct. Des. Tall Spec. Build.* **20**, 881–900. (doi:10.1002/tal.712)
178. Guo H, Zhang L, Zhang L, Zhou J. 2004 Optimal placement of sensors for structural health monitoring using improved genetic algorithms. *Smart Mater. Struct.* **13**, 528. (doi:10.1088/0964-1726/13/3/011)
179. Cantero-Chinchilla S, Aranguren G, Royo JM, Chiachío M, Etxaniz J, Calvo-Echenique A. 2021 Structural health monitoring using ultrasonic guided-waves and the degree of health index. *Sensors* **21**, 993. (doi:10.3390/s21030993)
180. Li M, Kefal A, Cerik B, Oterkus E. 2019 Structural health monitoring of submarine pressure hull using inverse finite element method. In *Trends in the analysis and design of marine structures: Proc. 7th Int. Conf. on Marine Structures (MARSTRUCT 2019, Dubrovnik, Croatia, 6–8 May 2019)*, p. 293. New York, NY: CRC Press.
181. Shen Y. 2014 Structural health monitoring using linear and nonlinear ultrasonic guided waves. PhD thesis. University of South Carolina, Columbia, SC, USA.
182. Srivastava A, Lanza di Scalea F. 2010 Quantitative structural health monitoring by ultrasonic guided waves. *J. Eng. Mech.* **136**, 937–944. (doi:10.1061/(ASCE)EM.1943-7889.0000136)
183. Mitra M, Gopalakrishnan S. 2016 Guided wave based structural health monitoring: a review. *Smart Mater. Struct.* **25**, 053001. (doi:10.1088/0964-1726/25/5/053001)
184. Eiras J, Kundu T, Popovics JS, Monzó J, Soriano L, Payá J. 2014 Evaluation of frost damage in cement-based materials by a nonlinear elastic wave technique. In *Health monitoring of structural and biological systems 2014*, vol. 9064, p. 90641G. International Society for Optics and Photonics.
185. Giurgiutiu V. 2005 Tuned Lamb wave excitation and detection with piezoelectric wafer active sensors for structural health monitoring. *J. Intell. Mater. Syst. Struct.* **16**, 291–305. (doi:10.1177/1045389X05050106)
186. Shin SW, Yun CB, Popovics JS, Kim JH. 2007 Improved Rayleigh wave velocity measurement for nondestructive early-age concrete monitoring. *Res. Nondestr. Eval.* **18**, 45–68. (doi:10.1080/09349840601128762)
187. Xu B, Giurgiutiu V. 2007 Single mode tuning effects on Lamb wave time reversal with piezoelectric wafer active sensors for structural health monitoring. *J. Nondestr. Eval.* **26**, 123–134. (doi:10.1007/s10921-007-0027-8)
188. Wang CH, Rose JT, Chang FK. 2004 A synthetic time-reversal imaging method for structural health monitoring. *Smart Mater. Struct.* **13**, 415. (doi:10.1088/0964-1726/13/2/020)
189. Moll J, Fritzen CP. 2010 Time-varying inverse filtering for high resolution imaging with ultrasonic guided waves. In *10th European Conf. on Non-Destructive Testing*, pp. 1–10.
190. He J, Rocha DC, Sava P. 2020 Guided wave tomography based on least-squares reverse-time migration. *Struct. Health Monit.* **19**, 1237–1249. (doi:10.1177/1475921719880296)

191. He J, Leckey CA, Leser PE, Leser WP. 2019 Multi-mode reverse time migration damage imaging using ultrasonic guided waves. *Ultrasonics* **94**, 319–331. (doi:10.1016/j.ultras.2018.08.005)
192. Zhao M, Zhou W, Huang Y, Li H. 2020 Sparse Bayesian learning approach for propagation distance recognition and damage localization in plate-like structures using guided waves. *Struct. Health Monit.* **20**, 1475921720902277. (doi:10.1177/1475921720902277)
193. Lu X, Lu M, Zhou LM, Su Z, Cheng L, Ye L, Meng G. 2010 Evaluation of welding damage in welded tubular steel structures using guided waves and a probability-based imaging approach. *Smart Mater. Struct.* **20**, 015018. (doi:10.1088/0964-1726/20/1/015018)
194. Smyl D, Tallman TN, Black JA, Hauptmann A, Liu D. 2021 Learning and correcting non-Gaussian model errors. *J. Comput. Phys.* **432**, 110152. (doi:10.1016/j.jcp.2021.110152)
195. Yuan FG, Zargar SA, Chen Q, Wang S. 2020 Machine learning for structural health monitoring: challenges and opportunities. In *Sensors and smart structures technologies for civil, mechanical, and aerospace systems 2020*, vol. 11379, p. 1137903. International Society for Optics and Photonics.
196. Finotti RP, Cury AA, Barbosa FdS. 2019 An SHM approach using machine learning and statistical indicators extracted from raw dynamic measurements. *Latin Am. J. Solids Struct.* **16**, 1–17. (doi:10.1590/1679-78254942)
197. Khuc T, Catbas FN. 2017 Completely contactless structural health monitoring of real-life structures using cameras and computer vision. *Struct. Control Health Monit.* **24**, e1852. (doi:10.1002/stc.1852)
198. Feng MQ, Fukuda Y, Feng D, Mizuta M. 2015 Nontarget vision sensor for remote measurement of bridge dynamic response. *J. Bridge Eng.* **20**, 04015023. (doi:10.1061/(ASCE)BE.1943-5592.0000747)
199. Luo L, Feng MQ, Wu ZY. 2018 Robust vision sensor for multi-point displacement monitoring of bridges in the field. *Eng. Struct.* **163**, 255–266. (doi:10.1016/j.engstruct.2018.02.014)
200. Yoon H, Elanwar H, Choi H, Golparvar-Fard M, Spencer Jr BF. 2016 Target-free approach for vision-based structural system identification using consumer-grade cameras. *Struct. Control Health Monit.* **23**, 1405–1416. (doi:10.1002/stc.1850)
201. Yang Y, Dorn C, Mancini T, Talken Z, Kenyon G, Farrar C, Mascareñas D. 2017 Blind identification of full-field vibration modes from video measurements with phase-based video motion magnification. *Mech. Syst. Signal Process.* **85**, 567–590. (doi:10.1016/j.ymssp.2016.08.041)
202. Dong CZ, Bas S, Catbas FN. 2019 A completely non-contact recognition system for bridge unit influence line using portable cameras and computer vision. *Smart Struct. Syst.* **24**, 617–630. (doi:10.12989/sss.2019.24.5.617)
203. Jana D, Nagarajaiah S. 2021 Computer vision-based real-time cable tension estimation in Dubrovnik cable-stayed bridge using moving handheld video camera. *Struct. Control Health Monit.* **28**, e2713. (doi:10.1002/stc.2713)
204. Liu Z, Cao Y, Wang Y, Wang W. 2019 Computer vision-based concrete crack detection using U-net fully convolutional networks. *Autom. Constru.* **104**, 129–139. (doi:10.1016/j.autcon.2019.04.005)
205. Gao Y, Mosalam KM. 2018 Deep transfer learning for image-based structural damage recognition. *Comput.-Aided Civil Infrastructure Eng.* **33**, 748–768. (doi:10.1111/mice.12363)
206. Shen HK, Chen PH, Chang LM. 2018 Human-visual-perception-like intensity recognition for color rust images based on artificial neural network. *Autom. Constru.* **90**, 178–187. (doi:10.1016/j.autcon.2018.02.023)
207. Pauly L, Hogg D, Fuentes R, Peel H. 2017 Deeper networks for pavement crack detection. In *Proc. 34th ISARC*, pp. 479–485. IAARC.
208. Cha YJ, Choi W, Büyüköztürk O. 2017 Deep learning-based crack damage detection using convolutional neural networks. *Comput.-Aided Civil Infrastructure Eng.* **32**, 361–378. (doi:10.1111/mice.12263)
209. Dung CV. 2019 Autonomous concrete crack detection using deep fully convolutional neural network. *Autom. Constru.* **99**, 52–58. (doi:10.1016/j.autcon.2018.11.028)
210. Chen FC, Jahanshahi MR. 2017 NB-CNN: deep learning-based crack detection using convolutional neural network and naïve Bayes data fusion. *IEEE Trans. Ind. Electron.* **65**, 4392–4400. (doi:10.1109/TIE.2017.2764844)

211. Cha YJ, You K, Choi W. 2016 Vision-based detection of loosened bolts using the Hough transform and support vector machines. *Autom. Constru.* **71**, 181–188. (doi:10.1016/j.autcon.2016.06.008)
212. Huynh TC, Park JH, Jung HJ, Kim JT. 2019 Quasi-autonomous bolt-loosening detection method using vision-based deep learning and image processing. *Autom. Constru.* **105**, 102844. (doi:10.1016/j.autcon.2019.102844)
213. Cha YJ, Choi W, Suh G, Mahmoudkhani S, Büyüköztürk O. 2018 Autonomous structural visual inspection using region-based deep learning for detecting multiple damage types. *Comput.-Aided Civil Infrastruct. Eng.* **33**, 731–747. (doi:10.1111/mice.12334)
214. Kong X, Li J. 2019 Non-contact fatigue crack detection in civil infrastructure through image overlapping and crack breathing sensing. *Autom. Constru.* **99**, 125–139. (doi:10.1016/j.autcon.2018.12.011)
215. Kong X, Li J. 2018 Image registration-based bolt loosening detection of steel joints. *Sensors* **18**, 1000. (doi:10.3390/s18041000)
216. Dominici D, Alicandro M, Massimi V. 2017 UAV photogrammetry in the post-earthquake scenario: case studies in L'Aquila. *Geomatics, Natural Hazards Risk* **8**, 87–103. (doi:10.1080/19475705.2016.1176605)
217. Choi J, Yeum CM, Dyke SJ, Jahanshahi MR. 2018 Computer-aided approach for rapid post-event visual evaluation of a building facade. *Sensors* **18**, 3017. (doi:10.3390/s18093017)
218. Buffi G, Manciola P, Grassi S, Barberini M, Gambi A. 2017 Survey of the Ridracoli Dam: UAV-based photogrammetry and traditional topographic techniques in the inspection of vertical structures. *Geomatics, Nat. Hazards Risk* **8**, 1562–1579. (doi:10.1080/19475705.2017.1362039)
219. Khaloo A, Lattanzi D, Jachimowicz A, Devaney C. 2018 Utilizing UAV and 3D computer vision for visual inspection of a large gravity dam. *Front. Built Environ.* **4**, 31. (doi:10.3389/fbuil.2018.00031)
220. Özaslan T, Shen S, Mulgaonkar Y, Michael N, Kumar V. 2015 Inspection of penstocks and featureless tunnel-like environments using micro UAVs. In *Field and service robotics*, pp. 123–136. New York, NY: Springer.
221. Banić M, Miltenović A, Pavlović M, Ćirić I. 2019 Intelligent machine vision based railway infrastructure inspection and monitoring using UAV. *Facta Universitatis, Series: Mech. Eng.* **17**, 357–364. (doi:10.22190/FUME190507041B)
222. Shao J, Tang L, Liu M, Shao G, Sun L, Qiu Q. 2020 BDD-Net: a general protocol for mapping buildings damaged by a wide range of disasters based on satellite imagery. *Remote Sensing* **12**, 1670. (doi:10.3390/rs12101670)
223. Gupta R, Shah M. 2021 Rescuenet: joint building segmentation and damage assessment from satellite imagery. In *2020 25th Int. Conf. on Pattern Recognition (ICPR)*, pp. 4405–4411. IEEE.
224. Furukawa Y, Hernández C. 2015 Multi-view stereo: a tutorial. *Foundations and Trends® in Computer Graphics and Vision* **9**, 1–148. (doi:10.1561/0600000052)
225. Braun A, Borrmann A. 2019 Combining inverse photogrammetry and BIM for automated labeling of construction site images for machine learning. *Autom. Constru.* **106**, 102879. (doi:10.1016/j.autcon.2019.102879)
226. Stavroulaki M, Riveiro B, Drosopoulos GA, Solla M, Koutsianitis P, Stavroulakis GE. 2016 Modelling and strength evaluation of masonry bridges using terrestrial photogrammetry and finite elements. *Adv. Eng. Softw.* **101**, 136–148. (doi:10.1016/j.advengsoft.2015.12.007)
227. Zollini S, Alicandro M, Dominici D, Quaresima R, Giallonardo M. 2020 UAV photogrammetry for concrete bridge inspection using object-based image analysis (OBIA). *Remote Sens.* **12**, 3180. (doi:10.3390/rs12193180)
228. Leishear RA. 2021 Bridge safety dangers-fatigue cracks, brittle failures and grit blasting. *J. Civil, Constru. Environ. Eng.* **6**, 28–45. (doi:10.11648/j.jccee.20210602.12)
229. Wagg D, Worden K, Barthorpe R, Gardner P. 2020 Digital twins: state-of-the-art and future directions for modeling and simulation in engineering dynamics applications. *ASCE-ASME J. Risk Uncert. Eng. Syst. Part B Mech. Eng.* **6**, 030901. (doi:10.1115/1.4046739)
230. Seshadri BR, Krishnamurthy T. 2017 Structural health management of damaged aircraft structures using digital twin concept. In *25th AIAA/AHS Adaptive Structures Conf.*, p. 1675.
231. Evensen G. 2018 Analysis of iterative ensemble smoothers for solving inverse problems. *Comput. Geosci.* **22**, 885–908. (doi:10.1007/s10596-018-9731-y)
232. Iglesias MA, Law KJ, Stuart AM. 2013 Ensemble Kalman methods for inverse problems. *Inverse Prob.* **29**, 045001. (doi:10.1088/0266-5611/29/4/045001)

233. Seppänen A, Vauhkonen M, Vauhkonen P, Somersalo E, Kaipio J. 2001 State estimation with fluid dynamical evolution models in process tomography—an application to impedance tomography. *Inverse Prob.* **17**, 467. (doi:10.1088/0266-5611/17/3/307)
234. Lunz S, Hauptmann A, Tarvainen T, Schönlieb CB, Arridge S. 2021 On learned operator correction in inverse problems. *SIAM J. Imag. Sci.* **14**, 92–127. (doi:10.1137/20M1338460)
235. Huttunen JM, Kaipio JP. 2007 Approximation errors in nonstationary inverse problems. *Inverse Probl. Imag.* **1**, 77. (doi:10.3934/ipi.2007.1.77)
236. Benning M, Burger M. 2018 Modern regularization methods for inverse problems. *Acta Numerica* **27**, 1–111. (doi:10.1017/S0962492918000016)
237. Lieberman C, Willcox K, Ghattas O. 2010 Parameter and state model reduction for large-scale statistical inverse problems. *SIAM J. Sci. Comput.* **32**, 2523–2542. (doi:10.1137/090775622)
238. Nagel WE, Resch MM, Kroner DB. 2019 *High performance computing in science and engineering*. New York, NY: Springer.
239. Gaska K, Generowicz A, Zimoch I, Ciuła J, Iwanicka Z. 2018 A high-performance computing (HPC) based integrated multithreaded model predictive control (MPC) for water supply networks. *Arch., Civil Eng., Environ.* **10**, 141–151. (doi:10.21307/acee-2017-058)
240. Saibaba AK, Bakhos T, Kitanidis PK. 2013 A flexible Krylov solver for shifted systems with application to oscillatory hydraulic tomography. *SIAM J. Sci. Comput.* **35**, A3001–A3023. (doi:10.1137/120902690)
241. Yang Y, Grover P, Kar S. 2017 Coded distributed computing for inverse problems. In *Proc. 31st Int. Conf. on Neural Information Processing Systems*, pp. 709–719.
242. Lucas A, Iliadis M, Molina R, Katsaggelos AK. 2018 Using deep neural networks for inverse problems in imaging: beyond analytical methods. *IEEE Signal Process Mag.* **35**, 20–36. (doi:10.1109/MSP.2017.2760358)
243. Avilés F, Oliva-Avilés AI, Cen-Puc M. 2018 Piezoresistivity, strain, and damage self-sensing of polymer composites filled with carbon nanostructures. *Adv. Eng. Mater.* **20**, 1701159. (doi:10.1002/adem.201701159)
244. Han B, Ding S, Yu X. 2015 Intrinsic self-sensing concrete and structures: a review. *Measurement* **59**, 110–128. (doi:10.1016/j.measurement.2014.09.048)
245. Han J, Pan J, Cai J, Li X. 2020 A review on carbon-based self-sensing cementitious composites. *Constru. Build. Mater.* **265**, 120764. (doi:10.1016/j.conbuildmat.2020.120764)
246. Forintos N, Czigany T. 2019 Multifunctional application of carbon fiber reinforced polymer composites: electrical properties of the reinforcing carbon fibers–a short review. *Composit. Part B: Eng.* **162**, 331–343. (doi:10.1016/j.compositesb.2018.10.098)
247. Tallman TN, Smyl DJ. 2020 Structural health and condition monitoring via electrical impedance tomography in self-sensing materials: a review. *Smart Mater. Struct.* **29**, 123001. (doi:10.1088/1361-665X/abb352)
248. Wang D, Chung D. 2013 Through-thickness piezoresistivity in a carbon fiber polymer-matrix structural composite for electrical-resistance-based through-thickness strain sensing. *Carbon* **60**, 129–138. (doi:10.1016/j.carbon.2013.04.005)
249. Koecher MC, Pande JH, Merkley S, Henderson S, Fullwood DT, Bowden AE. 2015 Piezoresistive in-situ strain sensing of composite laminate structures. *Compos. Part B: Eng.* **69**, 534–541. (doi:10.1016/j.compositesb.2014.09.029)
250. Ku-Herrera JdJ, La Saponara V, Avilés F. 2018 Selective damage sensing in multiscale hierarchical composites by tailoring the location of carbon nanotubes. *J. Intell. Mater. Syst. Struct.* **29**, 553–562. (doi:10.1177/1045389X17711790)
251. Hou TC, Loh KJ, Lynch JP. 2007 Spatial conductivity mapping of carbon nanotube composite thin films by electrical impedance tomography for sensing applications. *Nanotechnology* **18**, 315501. (doi:10.1088/0957-4484/18/31/315501)
252. Groo L, Nasser J, Inman D, Sodano H. 2021 Fatigue damage tracking and life prediction of fiberglass composites using a laser induced graphene interlayer. *Composite Part B: Eng.* **218**, 108935. (doi:10.1016/j.compositesb.2021.108935)
253. Groo L, Nasser J, Inman D, Sodano H. 2021 Damage localization in fiberglass-reinforced composites using laser induced graphene. *Smart Mater. Struct.* **30**, 035006. (doi:10.1088/1361-665X/abdc0c)
254. Talamadupula KK, Povolny S, Prakash N, Seidel GD. 2021 Piezoresistive detection of simulated hotspots and the effects of low velocity impact at the mesoscale in nanocomposite bonded energetic materials via multiphysics peridynamics modeling. *Comput. Mater. Sci.* **188**, 110211. (doi:10.1016/j.commatsci.2020.110211)

255. Talamadupula KK, Povolny SJ, Prakash N, Seidel GD. 2020 Mesoscale strain and damage sensing in nanocomposite bonded energetic materials under low velocity impact with frictional heating via peridynamics. *Model. Simul. Mater. Sci. Eng.* **28**, 085011. (doi:10.1088/1361-651X/abbfb9)
256. Yoo DY, You I, Lee SJ. 2018 Electrical and piezoresistive sensing capacities of cement paste with multi-walled carbon nanotubes. *Arch. Civil Mech. Eng.* **18**, 371–384. (doi:10.1016/j.acme.2017.09.007)
257. Ricohermoso III E, Rosenburg F, Klug F, Nicoloso N, Schlaak HF, Riedel R, Ionescu E. 2021 Piezoresistive carbon-containing ceramic nanocomposites–a review. *Open Ceramics* **5**, 100057. (doi:10.1016/j.oceram.2021.100057)
258. McCrary-Dennis MC, Okoli OI. 2012 A review of multiscale composite manufacturing and challenges. *J. Reinf. Plast. Compos.* **31**, 1687–1711. (doi:10.1177/0731684412456612)
259. Ma PC, Siddiqui NA, Marom G, Kim JK. 2010 Dispersion and functionalization of carbon nanotubes for polymer-based nanocomposites: a review. *Compos. Part A: Appl. Sci. Manuf.* **41**, 1345–1367. (doi:10.1016/j.compositesa.2010.07.003)
260. Gong S, Zhu ZH. 2014 On the mechanism of piezoresistivity of carbon nanotube polymer composites. *Polymer* **55**, 4136–4149. (doi:10.1016/j.polymer.2014.06.024)
261. Hu N, Karube Y, Yan C, Masuda Z, Fukunaga H. 2008 Tunneling effect in a polymer/carbon nanotube nanocomposite strain sensor. *Acta Mater.* **56**, 2929–2936. (doi:10.1016/j.actamat.2008.02.030)
262. Lee BM, Loh KJ. 2015 A 2D percolation-based model for characterizing the piezoresistivity of carbon nanotube-based films. *J. Mater. Sci.* **50**, 2973–2983. (doi:10.1007/s10853-015-8862-y)
263. Alian A, Meguid S. 2019 Multiscale modeling of the coupled electromechanical behavior of multifunctional nanocomposites. *Compos. Struct.* **208**, 826–835. (doi:10.1016/j.compstruct.2018.10.066)
264. Ren X, Chaurasia AK, Oliva-Avilés AI, Ku-Herrera JJ, Seidel GD, Avilés F. 2015 Modeling of mesoscale dispersion effect on the piezoresistivity of carbon nanotube-polymer nanocomposites via 3D computational multiscale micromechanics methods. *Smart Mater. Struct.* **24**, 065031. (doi:10.1088/0964-1726/24/6/065031)
265. Talamadupula KK, Seidel GD. 2021 Statistical analysis of effective electro-mechanical properties and percolation behavior of aligned carbon nanotube/polymer nanocomposites via computational micromechanics. *Comput. Mater. Sci.* **197**, 110616. (doi:10.1016/j.commatsci.2021.110616)
266. Cattin C, Hubert P. 2014 Piezoresistance in polymer nanocomposites with high aspect ratio particles. *ACS Appl. Mater. Interfaces* **6**, 1804–1811. (doi:10.1021/am404808u)
267. Tallman T, Wang K. 2013 An arbitrary strains carbon nanotube composite piezoresistivity model for finite element integration. *Appl. Phys. Lett.* **102**, 011909. (doi:10.1063/1.4774294)
268. Koo G, Tallman T. 2020 Higher-order resistivity-strain relations for self-sensing nanocomposites subject to general deformations. *Compos. Part B: Eng.* **190**, 107907. (doi:10.1016/j.compositesb.2020.107907)
269. Bao W, Meguid S, Zhu Z, Weng G. 2012 Tunneling resistance and its effect on the electrical conductivity of carbon nanotube nanocomposites. *J. Appl. Phys.* **111**, 093726. (doi:10.1063/1.4716010)
270. Taya M, Kim W, Ono K. 1998 Piezoresistivity of a short fiber/elastomer matrix composite. *Mech. Mater.* **28**, 53–59. (doi:10.1016/S0167-6636(97)00064-1)
271. Zhao Y, Gschossmann S, Schagerl M, Gruener P, Kralovec C. 2018 Characterization of the spatial elastoresistivity of inkjet-printed carbon nanotube thin films. *Smart Mater. Struct.* **27**, 105009. (doi:10.1088/1361-665X/aad8f1)
272. Gruener P, Zhao Y, Schagerl M. 2017 Characterization of the spatial elastoresistivity of inkjet-printed carbon nanotube thin films for strain-state sensing. In *Nondestructive characterization and monitoring of advanced materials, aerospace, and civil infrastructure 2017*, vol. 10169, p. 101690F. International Society for Optics and Photonics.
273. Bay BK. 2008 Methods and applications of digital volume correlation. *J. Strain Anal. Eng. Des.* **43**, 745–760. (doi:10.1243/03093247JSA436)
274. Tallman T, Gungor S, Koo G, Bakis C. 2017 On the inverse determination of displacements, strains, and stresses in a carbon nanofiber/polyurethane nanocomposite from conductivity data obtained via electrical impedance tomography. *J. Intell. Mater. Syst. Struct.* **28**, 1–13. (doi:10.1177/1045389X17692053)

275. Hassan H, Tallman TN. 2020 Failure prediction in self-sensing nanocomposites via genetic algorithm-enabled piezoresistive inversion. *Struct. Health Monit.* **19**, 765–780. (doi:10.1177/1475921719863062)
276. Dowrick T, Holder D. 2018 Phase division multiplexed EIT for enhanced temporal resolution. *Physiol. Meas.* **39**, 034005. (doi:10.1088/1361-6579/aaad59)
277. Loh KJ, Hou TC, Lynch JP, Kotov NA. 2009 Carbon nanotube sensing skins for spatial strain and impact damage identification. *J. Nondestr. Eval.* **28**, 9–25. (doi:10.1007/s10921-009-0043-y)
278. Dai H, Thostenson ET. 2019 Large-area carbon nanotube-based flexible composites for ultra-wide range pressure sensing and spatial pressure mapping. *ACS Appl. Mater. Interfaces* **11**, 48 370–48 380. (doi:10.1021/acsami.9b17100)
279. Nayak S, Das S. 2019 Spatial damage sensing ability of metallic particulate-reinforced cementitious composites: insights from electrical resistance tomography. *Mater. Des.* **175**, 107817. (doi:10.1016/j.matdes.2019.107817)
280. Gupta S, Gonzalez JG, Loh KJ. 2017 Self-sensing concrete enabled by nano-engineered cement-aggregate interfaces. *Struct. Health Monit.* **16**, 309–323. (doi:10.1177/1475921716643867)
281. Tallman T, Wang K. 2016 An inverse methodology for calculating strains from conductivity changes in piezoresistive nanocomposites. *Smart Mater. Struct.* **25**, 115046. (doi:10.1088/0964-1726/25/11/115046)
282. Hassan H, Tallman TN. 2020 A comparison of metaheuristic algorithms for solving the piezoresistive inverse problem in self-sensing materials. *IEEE Sensors J.* **21**, 659–666. (doi:10.1109/JSEN.2020.3014554)
283. Ghaednia H, Owens CE, Keiderling LE, Varadarajan KM, Hart AJ, Schwab JH, Tallman TT. 2020 Is machine learning able to detect and classify failure in piezoresistive bone cement based on electrical signals? (http://arxiv.org/abs/201012147).
284. Zhao L, Tallman T, Lin G. 2020 Spatial damage characterization in self-sensing materials via neural network-aided electrical impedance tomography: a computational study. (http://arxiv.org/abs/201001674)
285. Hassan H, Tallman T. 2021 Precise damage shaping in self-sensing composites using electrical impedance tomography and genetic algorithms. (https://arxiv.org/abs/2112.04419)
286. Holder DS. 2004 *Electrical impedance tomography: methods, history and applications*. New York, NY: CRC Press.
287. Weinan E. 2021 The dawning of a new era in applied mathematics. *Not. Am. Math. Soc.* **68**, 565–571.
288. Han J, Jentzen A, Weinan E. 2018 Solving high-dimensional partial differential equations using deep learning. *Proc. Natl Acad. Sci. USA* **115**, 8505–8510. (doi:10.1073/pnas.1718942115)
289. Sun H, Burton HV, Huang H. 2020 Machine learning applications for building structural design and performance assessment: state-of-the-art review. *J. Build. Eng.* **33**, 101816. (doi:10.1016/j.jobe.2020.101816)
290. Lee S, Ha J, Zokhirova M, Moon H, Lee J. 2018 Background information of deep learning for structural engineering. *Arch. Comput. Methods Eng.* **25**, 121–129. (doi:10.1007/s11831-017-9237-0)
291. Simon HA. 1996 *The sciences of the artificial*, 3rd edn. New York, NY: The MIT Press.
292. Schon DA. 1983 *Reflective practitioner*, vol. 5126. New York, NY: Basic Books.
293. Buchanan R. 1992 Wicked problems in design thinking. *Design issues* **8**, 5–21. (doi:10.2307/1511637)
294. Badue C *et al.* 2020 Self-driving cars: a survey. *Expert Syst. Appl.* **165**, 113816. (doi:10.1016/j.eswa.2020.113816)
295. Mitchell T. 1997 *Machine learning*. New York, NY: McGraw Hill.
296. Ochoa KS, Ohlbrock PO, D'Acunto P, Moosavi V. 2020 Beyond typologies, beyond optimization: exploring novel structural forms at the interface of human and machine intelligence. *Int. J. Archit. Comput.* **19**, 1478077120943062. (doi:10.1177/1478077120943062)
297. Zheng H, Moosavi V, Akbarzadeh M. 2020 Machine learning assisted evaluations in structural design and construction. *Autom. Constru.* **119**, 103346. (doi:10.1016/j.autcon.2020.103346)
298. Wang M, Poulsen E, Reynolds D, Otani R. 2018 Conceptual stage predictive and collaborative design using machine learning. In *Proc. of IASS Annual Symposia*, vol. 2018, pp. 1–7. International Association for Shell and Spatial Structures (IASS).

299. Lipponen A, Huttunen JM, Romakkaniemi S, Kokkola H, Kolehmainen V. 2018 Correction of model reduction errors in simulations. *SIAM J. Sci. Comput.* **40**, B305–B327. (doi:10.1137/15M1052421)
300. Kaipio J, Somersalo E. 2007 Statistical inverse problems: discretization, model reduction and inverse crimes. *J. Comput. Appl. Math.* **198**, 493–504. (doi:10.1016/j.cam.2005.09.027)
301. Arridge SR, Kaipio JP, Kolehmainen V, Schweiger M, Somersalo E, Tarvainen T, Vauhkonen M. 2006 Approximation errors and model reduction with an application in optical diffusion tomography. *Inverse Prob.* **22**, 175–195. (doi:10.1088/0266-5611/22/1/010)
302. Koponen J, Lähivaara T, Kaipio J, Vauhkonen M. 2021 Model reduction in acoustic inversion by artificial neural network. (http://arxiv.org/abs/210502225).
303. Banert S, Ringh A, Adler J, Karlsson J, Oktem O. 2020 Data-driven nonsmooth optimization. *SIAM J. Optim.* **30**, 102–131. (doi:10.1137/18M1207685)
304. Wang Y, Sun Y, Liu Z, Sarma SE, Bronstein MM, Solomon JM. 2019 Dynamic graph CNN for learning on point clouds. *ACM Trans. Graph.* **38**, 1–12.
305. Herzberg W, Rowe DB, Hauptmann A, Hamilton SJ. 2021 Graph convolutional networks for model-based learning in nonlinear inverse problems. *IEEE Trans. Comput. Imaging* **7**, 1341–1353. (doi:10.1109/TCI.2021.3132190)
306. Froyd JE, Wankat PC, Smith KA. 2012 Five major shifts in 100 years of engineering education. *Proc. IEEE* **100**(Special Centennial Issue), 1344–1360. (doi:10.1109/JPROC.2012.2190167)
307. Bulleit WM. 2012 What makes an engineering education an engineering education? In *Structures congress 2012*, pp. 1143–1151.
308. Koen BV. 2013 Debunking contemporary myths concerning engineering. In *Philosophy and engineering: Reflections on practice, principles and process*, pp. 115–137. New York, NY: Springer.
309. Goldman SL. 2004 Why we need a philosophy of engineering: a work in progress. *Interdiscip. Sci. Rev.* **29**, 163–176. (doi:10.1179/030801804225012572)
310. Dym CL, Agogino AM, Eris O, Frey DD, Leifer LJ. 2005 Engineering design thinking, teaching, and learning. *J. Eng. Educ.* **94**, 103–120. (doi:10.1002/j.2168-9830.2005.tb00832.x)
311. Doridot F. 2008 Towards an 'Engineered epistemology'? *Interdiscip. Sci. Rev.* **33**, 254–262. (doi:10.1179/174327908X366941)
312. Rawat W, Wang Z. 2017 Deep convolutional neural networks for image classification: a comprehensive review. *Neural Comput.* **29**, 2352–2449. (doi:10.1162/neco_a_00990)
313. Vaswani A, Shazeer N, Parmar N, Uszkoreit J, Jones L, Gomez AN, Kaiser L, Polosukhin I. 2017 Attention is all you need. (http://arxiv.org/abs/170603762).
314. Wu Z, Pan S, Chen F, Long G, Zhang C, Philip SY. 2020 A comprehensive survey on graph neural networks. *IEEE Trans. Neural Netw. Learn. Syst.* **32**, 4–24. (doi:10.1109/TNNLS.2020.2978386)